

## Searching for Spatial Patterns in a Pollinator–Plant–Herbivore Mathematical Model

Faustino Sánchez-Garduño ·  
Víctor F. Breña-Medina

Received: 29 May 2008 / Accepted: 22 October 2010  
© Society for Mathematical Biology 2010

**Abstract** This paper deals with the spatio-temporal dynamics of a pollinator–plant–herbivore mathematical model. The full model consists of three nonlinear reaction–diffusion–advection equations defined on a rectangular region. In view of analyzing the full model, we firstly consider the temporal dynamics of three homogeneous cases. The first one is a model for a mutualistic interaction (pollinator–plant), later on a sort of predator–prey (plant–herbivore) interaction model is studied. In both cases, the interaction term is described by a Holling response of type II. Finally, by considering that the plant population is the unique feeding source for the herbivores, a mathematical model for the three interacting populations is considered. By incorporating a constant diffusion term into the equations for the pollinators and herbivores, we numerically study the spatiotemporal dynamics of the first two mentioned models. For the full model, a constant diffusion and advection terms are included in the equation for the pollinators. For the resulting model, we sketch the proof of the existence, positiveness, and boundedness of solution for an initial and boundary values problem. In order to see the separated effect of the diffusion and advection terms on the final population distributions, a set of numerical simulations are included. We used homogeneous Dirichlet and Neumann boundary conditions.

**Keywords** Pollinator–plant–herbivore mathematical models · Reaction–diffusion–advection equations · Existence · Positiveness and boundedness · Spatial patterns · Holling functional response of type II

---

F. Sánchez-Garduño (✉) · V.F. Breña-Medina  
Departamento de Matemáticas, Facultad de Ciencias, Universidad Nacional Autónoma de México (UNAM), Circuito Exterior, Ciudad Universitaria, México, 04510, DF, México  
e-mail: [faustino@servidor.unam.mx](mailto:faustino@servidor.unam.mx)

V.F. Breña-Medina  
e-mail: [victoranas@gmail.com](mailto:victoranas@gmail.com)

## 1 Introduction

The heterogeneity is one of the most obvious features of the environment. In fact, humidity, temperature, light, food and water distribution, vegetation, local weather, etc., are different from one location to another. The drastic changes in the weather during the year, originates migratory movements of biological populations, like the monarch butterfly from Canada and the US to the central west parts of Mexico during the winter. The population migratory movements are not at random, in fact, depend upon specific individuals; they form swarms, herds, flocks, or schools, for instance.

On the other hand, the gregarious or social behavior of some species is on the basis of the grouping of populations. That is, they defend themselves from other species, overcome hostile environmental conditions, mate, etc. The grouping of microscopical individuals also has been observed: the amoeba *Dictyostelium discoideum* exhibits spiral aggregative patterns toward those places of the medium where the emission of a chemoattractant (cAMP) takes place. The colonies of the bacteria *Bacillus subtilis* adopt different morphologies—included the branched patterns of fractal-like type—depending on the agar and nutrient concentrations in the Petri dish. Nevertheless, the underlying interplay in these processes is between the individual and the collective movement; in fact, the grouping processes involves different space and time scales. Consequently, questions such as how do the individuals interact with each other in order to produce such a collective ordered spatial distributions are crucial.

The formation of different aggregation and aggregation-like patterns in populations is the result of a complex nonlinear cooperative individual behavior—which includes short distances signaling, sounds, movements, among others. In Couzin and Krause (2003), the authors present a study for the formation of different types of self-organization processes in vertebrates. Additionally, the basis for the development of some mathematical models by describing different types of ecological populations aggregation is presented in Okubo (1986).

Depending upon the way how the spatial variables are incorporated into the models, these can be classified in two main families: discrete and continuous. The spatial discrete models include:

1. *Patches*. Here, the space is divided in regions or patches which, according to certain biological and/or physical features, can be seen as a whole. For each patch, the population interactions can be described by a system of ordinary differential equations (ODE) and the patches are coupled by diffusion which is characterized by the population flow between two adjacent patches. Moreover, for the simplest case, the magnitude is proportional to the corresponding population density difference per each patch. For instance, denoting by  $u_i^k(t)$  the population density of the population  $i$  at the patch  $k$  at time  $t$ , the ODE system

$$\begin{aligned}\dot{u}_1^k(t) &= f(u_1^k, u_2^k) + D_1(u_1^{k+1} - u_1^k), \\ \dot{u}_2^k(t) &= g(u_1^k, u_2^k) + D_2(u_2^{k+1} - u_2^k),\end{aligned}$$

with  $i = 1, 2$  and  $k = 1, 2, 3$  describes two interacting populations in a habitat with three patches. Here, the density dependent functions  $f$  and  $g$  denote the rate of

change of each population and  $D_i$  are positive constants. This idea can be generalized in order to consider the dynamics of more interacting populations in a patchy environment. In May and Southwood (1990), the reader will find a general view on this topic.

**2. Cellular automata.** The habitat is divided in discrete units called *cells* and the individuals movement appears in an indirect way: just by saying that the cell is occupied or unoccupied. The simplest cellular automaton consists of a: (i) finite one-dimensional discrete row, (ii) small universe of eligible states at which the cells can be, (iii) *rule of evolution* which tells us the criteria for updating the state of the  $j$ th cell at the *generation* (discrete)  $t$ , depending upon the neighboring cells state at the  $t - 1$  generation. The neighboring cells could be just the very closest ones (the first neighbors) or, additionally, those situated far away (long range neighbors). The evolution rule could take into account habitat ecological features, interaction with other species, and possibly the behavioral aspects of the individuals. Hence, denoting by  $u_j^{(k)}$  the  $j$ th cell state at  $k$  generation, a cellular automaton example is

$$u_j^{(k)} = F_j(u_{j-l}^{(k-1)}, \dots, u_{j-1}^{(k-1)}, u_j^{(k-1)}, u_{j+1}^{(k-1)}, \dots, u_{j+r}^{(k-1)}), \quad (1)$$

where the function  $F_j$  gives the evolution rule and  $u_j^{(k)}$  depends on the state of the  $r$  cells situated at the right and those  $l$  cells allocated to the left at the previous generation. Once the initial state (at  $t = 0$ ) is given, the automaton is updated accordingly to the law given by (1). This produces a two-dimensional landscape composed by a set of horizontal rows which gives the population spatial distribution at the corresponding cellular automaton generation. A readable, recent, and critic reference on this topic is given in Molofsky and Bever (2004).

**3. Coupled maps.** Discretization of continuous models provides an origin for these models. As a way of example, consider a finite one-dimensional habitat, where the population density,  $u(x, t)$ , satisfies the partial differential equation (PDE)  $u_t = Du_{xx} + f(u)$ , where  $(x, t) \in [a, b] \times (0, T]$  and  $f$  is the growth rate. Once the space and time intervals are discretized by:  $a = x_0, x_1, \dots, x_n = b$ , such that  $x_i - x_{i-1} = (b - a)/n \equiv h$  and by  $t_0 = 0, t_1, t_2, \dots, t_m = T$  where  $t_{j+1} - t_j = T/m \equiv k$ , respectively, and denoting by  $u_{i,j}$  the population density at  $(x_i, t_j)$ , a central difference pointwise approximation for the above PDE gives the *discrete coupled map*

$$u_{i,j+1} = u_{i,j} + r(u_{i-1,j} - 2u_{i,j} + u_{i+1,j}) + kh^2 f(u_{i,j}),$$

where  $r = kD/h^2$ . By using other types of approximations for the derivatives  $u_t$  and  $u_{xx}$ , also other coupled maps can be obtained.

Metapopulations is another family of discrete models which we will not describe here; we just mention that this approach has been applied for the study of natural or artificial fragmented habitats. Details on this topic can be seen in Hanski (1997, 1999) and Market (2002).

On the other side, the continuous spatial models include explicitly space variables, and according to space range, these can be divided in two classes:

1. *Local models.* Here, the models take the form of PDE. One family of these are the *reaction-diffusion-advection equations* (RDAE):

$$\frac{\partial u_j}{\partial t} = \nabla \cdot (D_j \nabla u_j) - \vec{v} \cdot \nabla u_j + f_j(u_1, u_2, \dots, u_n), \quad j = 1, 2, \dots, n, \quad (2)$$

where  $u_j(\vec{r}, t)$  denotes the population density of the  $j$ th population at the point  $\vec{r}$  at time  $t$ ;  $D_j$  is the dispersion coefficient of the corresponding population which might depend on the population density, space or time variables;  $\nabla u_j$  is the spatial gradient of the population density;  $\nabla \cdot$  denotes the space divergence operator;  $\vec{v}$  is a drift vector affecting the movement of the population due to different factors, for instance, wind or water streams in a river, and  $f_j$  is the density dependent population growth rate. In order to complete the mathematical problem, the initial and boundary value conditions must be included. Equations (2) can be derived by using two alternative approaches.

- *Continuous media.* In this approach, the population—as a whole—can be seen as a sort of fluid. Thus, the *mass conservation law* plus a specific law for the population flow,  $\vec{J}$ , (the simplest one is *Fick's law*:  $\vec{J} \propto -\nabla u_j$ ), can be used to derive system (2). At certain space scales of description, RDAE equations could be appropriate for the description of the spatiotemporal dynamics of interacting populations. In Holmes et al. (1994), Okubo and Levin (2001), and Sánchez-Garduño (2001), the authors present a review of this approach in an ecological context.
- *Random walks.* On the other hand, the state variable,  $p(\vec{r}, t)$ , is the probability of an individual is at point  $\vec{r}$  in a given habitat, at time  $t$ . For a one-dimensional habitat, the derivation goes as follows: splitting the habitat by a constant distance  $\lambda$  and time discretization by intervals of period  $\tau$ . Let  $R$ ,  $L$ , and  $N$  be the probability of moving to the right, to the left and no movement, respectively. Then, the probability of the event: “the individual is at  $x$  at time  $t$ ,” is decomposed as the sum of probabilities of three mutually excluding events.<sup>1</sup> The next step is to carry out the Taylor series of  $p(x - \lambda, t - \tau)$ ,  $p(x + \lambda, t - \tau)$  and  $p(x, t - \tau)$  around  $(x, t)$  up to leading terms and using the *diffusive approximation*, which allows us to pass to continuous space and time variables. At the end, a diffusion-advection equation for  $p$  is obtained. In this approach, the incorporation of spatial features of the habitat and perhaps some behavioral aspects of the individuals of the population is possible in the probabilities  $p$ ,  $R$ ,  $L$  or  $N$ . Skellam was a precursor of this approach in ecology (see Skellam 1951, 1973). Since his pioneering papers, more work has been carried out by other authors (see Okubo and Levin 2001; Sánchez-Garduño 2001, and Turchin 1998).

2. *Nonlocal models.* These models consider the influence of a population density over a long range in the habitat into the dynamics of local population density. Some of them take the form of *integrodifferential equations* (see Alt 1985) where the integral terms contain a *kernel* having a precise ecological interpretation.

<sup>1</sup>These are: “the individual is at  $x - \lambda$  at time  $t - \tau$  and move to the right,” “the individual is at  $x + \lambda$  at time  $t - \tau$  and move to the left” and “the individual is at  $x$  at time  $t - \tau$  and stay there.”

We should say that fundamental ecological phenomena such as dispersion (see Holmes et al. 1994 and Okubo and Levin 2001) segregation (García-Ramos et al. 2000) and aggregation (see Sánchez-Garduño et al. 2010 and Turchin and Kareiva 1989) of interacting populations lead to important, mathematical and interpretative problems.

The emergence of ordered structures is ubiquitous in biology covering a wide range of areas and spatial and time scales. Those include: fetal development, coats of mammals, pigmentation of shells, structure of social insects nests, collective swarms of bacteria, army ants, vegetation distributions in arid and semiarid zones, etc. In mathematical ecology, the pioneering work due to Kierstead and Slobodkin (see Kierstead and Slobodkin 1953) whom were interested in understanding the phytoplankton blowing up associated with the red tide which is quite poisonous for fishes. Apparently, phytoplankton growth is triggered by the local nutrient accumulation among other substances which favor the organic growth. Thus, denoting by  $u(x, t)$ , the phytoplankton population density at the point  $x$  at time  $t$ , they proposed the model  $u_t = Du_{xx} + ru$ , defined on the finite one-dimensional habitat  $(0, L)$  with  $u(0, t) = u(L, t) = 0$  for all  $t$ . The existence of a critical habitat size,  $L_c = \pi\sqrt{D/r}$ , is proven such that if  $L < L_c$  the phytoplankton population decreases going down to extinction, however, it increases for  $L > L_c$ ; that is, a blowing up phenomenon occurs. A few years later, Levin and Segel and Steele (see Levin and Segel 1976 and Steele 1974) proposed a mechanism as the responsible of the emergence of patches. They considered two populations: phytoplankton and zooplankton represented by  $P(x, t)$  and  $H(x, t)$  at point  $x$  and time  $t$ , respectively; additionally, a predator-prey interaction described by a Lotka–Volterra model is taken into account. Indeed, conditions for ordered spatial distributions having the form of patches were obtained according to their model. Indeed, they followed the seminal paper by the British mathematician Alan Mathison Turing (see Turing 1952), who proposed a morphogenetic mechanism based on the simultaneous occurrence of reaction of substances and diffusion of them. This specific mechanism occurs on the assumption of the existence of a homogeneous state which is stable to time perturbations but unstable to spatiotemporal perturbations. In fact, these two requirements impose conditions on the reactive (interaction) and the diffusive (dispersion) parts. Whenever they are fulfilled, the *turingian morphogenetic* mechanism is triggered to rise some asymptotic ordered spatial distributions of the morphogens, also called *Turing patterns*. Moreover, this mechanism has been used to describe a variety of emerging patterns in several systems. Many examples of biological systems where different type of patterns emerge can be found in Murray (2003).

In relation with the occurrence of Turing patterns in ecological systems, the mathematical ecologists Akira Okubo and Simon Levin, wrote (see Okubo and Levin 2001):

In general, a diffusion process in an ecosystem tends to give rise to an uniform density of population in space. As a consequence, it may be expected that diffusion, when it occurs, plays the general role of increasing stability in a system of mixed populations and resources . . . However, there is an important exception, known as “diffusion-induced instability” or “diffusion instability.” This exception might not be a rare event especially in aquatic systems. Herein, we shall explore the Turing effect in ecosystems.

The mathematical basis of the diffusive instability in ecology has been presented in detail by several authors. For instance, Segel and Jackson (1972) and Mimura et al. (1979) have made it for continuous models; on the other hand, time discrete diffusion driven instability models have been discussed by Kot and Schaffer (1986). Additionally, recent research on patterns emergence in ecology from a mathematical modelling point of view is also given by Malchow et al. (2007).

In this paper, we explore the existence of ordered spatiotemporal distributions in a pollinator–plant–herbivore mathematical model defined on a rectangular region. The model consists of three RDA equations. To begin with, we do this by considering two subsystems: pollinator–plant and herbivore–plant interactions. Finally, we study the full pollinator–plant–herbivore system. The material contained in this paper is organized as follows. Section 2 deals with the temporal and spatiotemporal dynamics of an extreme particular case: a pollinator–plant interaction. In Sect. 3 a herbivore–plant interaction model is considered. Section 4 contains our study of the full pollinator–plant–herbivore interaction mathematical model. In the final section, we summarize our findings and indicate future research directions. In addition, a couple of appendixes are included where the existence of a positive equilibrium for the full homogeneous system and a qualitative description<sup>2</sup> of the existence, positiveness, and boundedness of the solution of the initial and boundary value problem associated with the RDA system are given.

## 2 A Pollinator–Plant Model

The analysis we present here is carried out in two steps. Firstly, the temporal dynamics of a mutualistic interaction model is reviewed, where a pollinator and a plant populations are considered. Secondly, we incorporate the space component in the previous model and carry out some numerical simulations.

### 2.1 The Assumptions and the Model

It is accepted that the mutualistic interactions are ubiquitous in nature. However, when the amount of theoretical studies on predation or competition are compared with those on mutualism, it is found that the last one are just a few. In this lack, the review on mutualistic studies, due to Boucher (see Boucher 1982), is an excellent reference.

The underlying hypothesis of the mutualistic model we consider here are: (1) The pollinators, in addition of the nectar and pollen from the plants, have other limited sources of food, in other words, they are not vital for the pollinators the plants, (2) The plants are pollinized exclusively by this pollinator population, i.e., they are highly specialized and (3) The pollinator–plant interaction is described by a *Holling functional response of type II*.<sup>3</sup> In the present context, the pollinator rate of visits to plants

<sup>2</sup>In Sánchez-Garduño and Breña-Medina (2010), the authors present the proofs of the mathematical results described here.

<sup>3</sup>The concepts' functional and numerical responses had their origin in predator–prey interactions. Here, we are borrowing the term from these, simply by considering that the qualitative properties of the function describing the rate of visits per pollinator, are the same as those of the Holling response of type II.

per pollinator is limited. In fact, it must be a monotonic growing function for low plant population density but for big enough plant population density, such function has an asymptotic behavior toward a horizontal straight line representing the maximum rate of visits of plants per pollinator.

Let  $a(t)$  and  $p(t)$  be the population density of pollinator and plants at time  $t$ , respectively. One model which captures the above hypothesis is:

$$\begin{aligned} \dot{a} &= a(K - a) + \frac{ap}{1 + p}, \\ \dot{p} &= -\frac{p}{2} + \frac{ap}{1 + p}, \end{aligned} \quad (3)$$

where  $K$  is the bifurcation parameter which, in addition to be the pollinator population carrying capacity, it also represents a measure of the preference of the pollinators for its own food sources. As far we know, the model (3) was originally proposed by Soberón and Martínez del Río (see Soberón and Martínez del Río 1981). They proposed it on the basis of the feasible ecological interpretation of all the parameters and expressions appearing in their original formulation. Here, we just kept the fundamental parameter:  $K$ . A preliminary analysis of (3) is carried out in Soberón and Martínez del Río (1981).

## 2.2 The Temporal Dynamics

The dynamics associated with system (3) can be obtained by using an usual nonlinear dynamical approach. Parts of this analysis can be seen in Arrowsmith and Place (1998). The relative position of the nontrivial null-clines

$$p_1(a) = \frac{a - K}{K + 1 - a} \quad \text{and} \quad p_2(a) = 2a - 1,$$

of system (3), determinates its nontrivial equilibria in the first quadrant of the phase plane and the way in which they touch each other, gives the local phase portrait.

The values of  $a$  for which  $p_1(a) = p_2(a)$  are

$$a_1, a_2 = \frac{1}{2}[(K + 1) \pm \sqrt{(K + 1)^2 - 2}];$$

we set  $K^* = \sqrt{2} - 1$  and  $K_1 = 1/2$ . In terms of these critical parameter values, we summarize the temporal dynamics as follows:

1. Any solution of (3) starting from  $(a_0, p_0)$  with  $a_0 \geq 0$  and  $p_0 \geq 0$  is bounded and nonnegative for all  $t$ .
2. System (3) has not *closed trajectories*.
3. The points  $P_0 = (0, 0)$  and  $P_1 = (K, 0)$  are equilibria for all  $K > 0$ :  $P_0$  is a saddle point;  $P_1$  a local stable node for  $0 < K < K_1$ , nonhyperbolic for  $K = K_1$  and a saddle for  $K > K_1$ ; meanwhile, if  $0 < K < K^*$ ,  $P_1$  is a *global attractor* on  $\mathbb{R}_+^2$ , i.e., the plant's population becomes extinct.

4. Whenever  $K = K^*$ , there are three equilibria:  $P_0$ ,  $P_1$ , and  $P^* = (a^*, p^*) = (1/\sqrt{2}, \sqrt{2} - 1)$ . The last one is a *nonhyperbolic* point of *saddle-node* type and, depending upon both population densities, the species persist in equilibrium or the plants tend to extinction.
5. For  $K^* < K < K_1$ , two equilibrium points appear which come from the *bifurcation* of  $P^*$ , one is a saddle and the other is a stable node. Depending on the population densities, the species persist or the plants become extinct.
6. If  $K \geq K_1$ , the system has three equilibria:  $P_0$ ,  $P_1$ , and  $P_r$ . Here, the species persist by exhibiting a *global attractor*:  $P_r$  belonging  $\mathbb{R}_+^2$ .

As a consequence of item one, for small enough values of  $K$ , the pollinator population prefers its own food resources. Thus, the mutualistic interaction term, really becomes important for big values of the parameter  $K$ .

Figure 1 shows the phase portrait<sup>4</sup> of the system (3) for relevant parameter values.

### 2.3 The Spatiotemporal Model and the Simulations

Here, we take into account spatial effects under following hypothesis: (1) The pollinators population movement—at individual level—is at random, (2) The plants do not disperse, but its spatial distribution changes because of the interaction with the pollinators, and (3) The temporal dynamics is given by the system (3). One model reflecting these assumptions is:

$$\begin{aligned}\frac{\partial a}{\partial t} &= D\Delta a + a\left(1 - \frac{a}{K}\right) + \frac{ap}{1+p}, \\ \frac{\partial p}{\partial t} &= -\frac{1}{2}p + \frac{ap}{1+p}.\end{aligned}\tag{4}$$

Here,  $a(\vec{r}, t)$  and  $p(\vec{r}, t)$  denote the population densities respectively at point  $\vec{r}$  of the habitat at time  $t$ ,  $D > 0$  is the diffusivity of the pollinator population, and  $\Delta$  denotes the two-dimensional Laplacian operator.

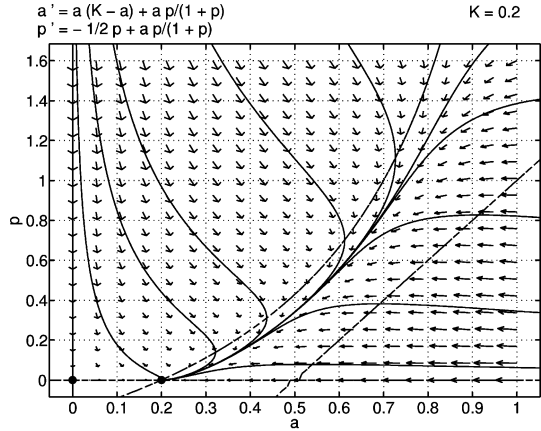
Given the ecological interpretation of the variables  $a$  and  $p$  in (4), positiveness and boundedness of the solution of an initial and boundary value problem associated with this system is imperative. We present an overview of the proof which gives sufficient conditions for a system which contains (4) in Appendix B. More details can be seen in Sánchez-Garduño and Breña-Medina (2010).

As complementary to the above mentioned study, we obtained the numerical solution of the nonlinear system (4), on the rectangular habitat  $\mathcal{R} = \{(x, y) | 0 < x < a, 0 < y < b\}$ , with initial conditions corresponding to a spatial perturbation of a stationary and homogeneous state of the system (4) and homogeneous Neumann boundary conditions. Figure 2 shows our findings<sup>5</sup> where the color scale in the spatiotemporal

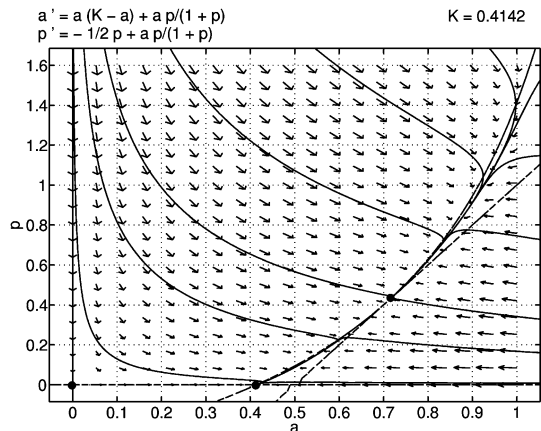
<sup>4</sup>All the phase portraits contained in this paper, were done by using the free *pplane* software developed by John C. Polking from Rice University.

<sup>5</sup>All the numerical solutions of the PDE systems we present in this paper were done by using the software *FlexPDE* which solves the system by using the finite element method.

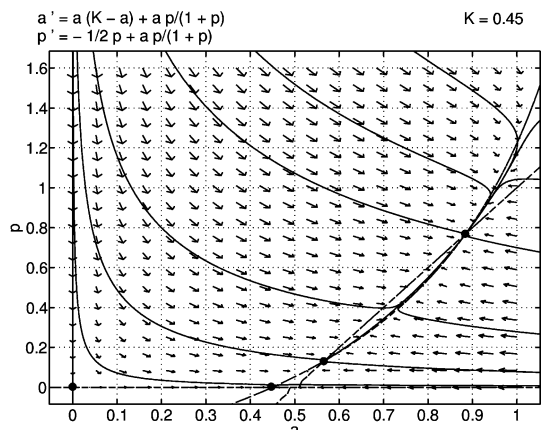
**Fig. 1** Phase portrait of the system (3) for different values of  $K$ . For the ecological interpretation of each one, see the text



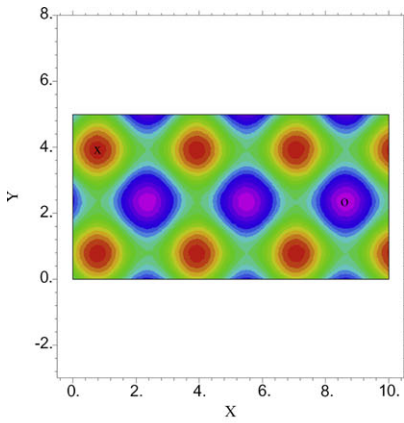
(a)  $K = 0.2 (K < K^*)$



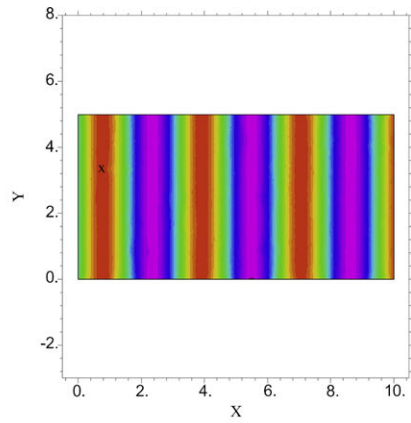
(b)  $K = K^* = \sqrt{2} - 1$



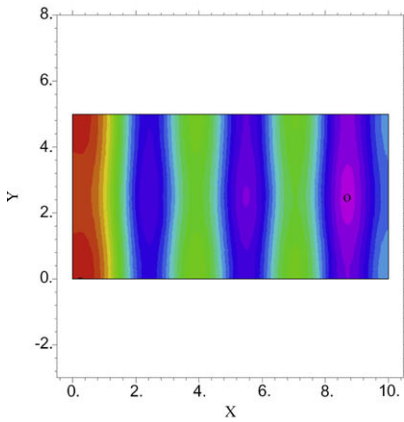
(c)  $K = 0.45 (K > K^*)$



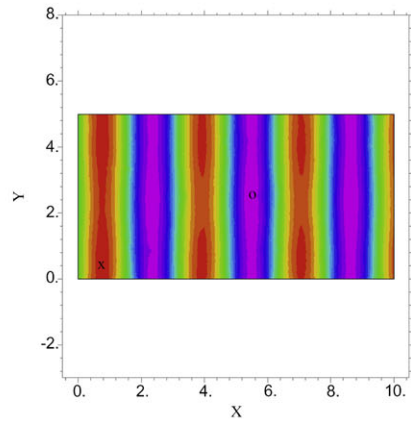
(a) The initial conditions: pollinator



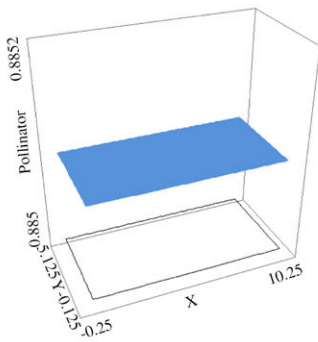
(b) The initial conditions: plant



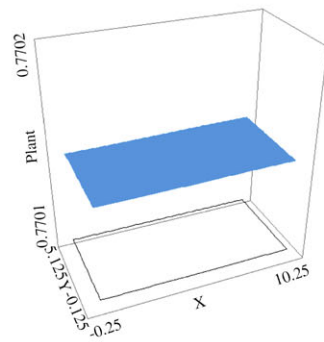
(c) Pollinator at  $t = 1.53$



(d) Plant at  $t = 1.53$



(e) The homogeneous final distribution: pollinator



(f) The homogeneous final distribution: plant

**Fig. 2** Numerical solutions of the system (4) at different running times

simulations we present along the paper follows the heat-like spectrum: red indicates the highest population density values and purple corresponds to the lowest values of the density.

In this case, the steady and homogeneous state of (4) given by the nontrivial equilibrium of the system (3), acts as an attractor in the space of solutions of the system, i.e., both population densities tend to the homogeneous spatial distribution as the time goes to infinity.

### 3 Other Extreme Case: Plant–Herbivore Interaction

Predation is one of the most studied (experimentally and theoretically) ecological interactions. Here, we consider one which, from a demographic perspective, can be seen as one of predator–prey type. For interpretation purposes, this takes the form of a plant–herbivore interaction.

#### 3.1 The Assumptions and the Model

We consider the following hypothesis: (1) The plants have limited sources and are the unique source of food for the herbivores, and (2) The plant–herbivore interaction is described by a functional response of type II.

Denoting by  $h(t)$  the herbivore population density at time  $t$ , a mathematical model which incorporates the above hypothesis is

$$\begin{aligned} \dot{p} &= p \left( 1 - \frac{p}{K} \right) - \frac{ph}{(1+p)}, \\ \dot{h} &= -\alpha\beta h + \beta \frac{ph}{(1+p)}, \end{aligned} \tag{5}$$

where  $\alpha$ ,  $\beta$ , and  $K$  are positive parameters.

#### 3.2 The Temporal Dynamics

The nontrivial null-clines of the system (5) are

$$h(p) = (1+p) \left( 1 - \frac{p}{K} \right) \quad \text{and} \quad p = \frac{\alpha}{1-\alpha},$$

with  $0 < \alpha < 1$ . The equilibria of the system (5) are

$$P_0 = (0, 0), \quad P_1 = (K, 0) \quad \text{and} \quad P_2 = (\bar{p}, \bar{h}),$$

where

$$\bar{p} = \frac{\alpha}{1-\alpha} \quad \text{and} \quad \bar{h} = (1 + \bar{p}) \left( 1 - \frac{\bar{p}}{K} \right).$$

Clearly,  $P_2$  exists in the positive quadrant depending on  $\bar{p}$  compared with  $K$ . We set

$$p^* = \frac{K - 1}{2} \quad \text{and} \quad \tilde{K}(\alpha) = \frac{1 + \alpha}{1 - \alpha}.$$

In what follows, we summarize the dynamics associated with the system (5). The proof of some results can be seen in Kot (2001) and Kuznetsov (2004).

The real part,  $\Re(\lambda_1, \lambda_2)$ , of the Jacobian matrix eigenvalues of (5) at  $P_2$  is

$$\Re(\lambda_1, \lambda_2) = \alpha h'(\bar{p}),$$

which given that  $0 < \alpha < 1$ , changes its sign, depending upon  $h'(\bar{p})$ .

Observe the following cases:

1. If  $K \leq \alpha/(1 - \alpha)$ , the herbivore population becomes extinct and that of the plants, stabilizes at  $P_1$ . This point can be a stable node or a saddle-node;
2. If  $K > \alpha/(1 - \alpha)$ ,  $P_1$  is a saddle point. Moreover, as can be seen,  $\tilde{K}(\alpha)$  plays an important role:
  - If  $K < \tilde{K}(\alpha)$ ,  $P_2$  is asymptotically stable and both species persist through a global attractor in  $\mathbb{R}_+^2$ . For example, through damped oscillations.
  - If  $K \geq \tilde{K}(\alpha)$ ,  $P_2$  is unstable and the populations coexist. Both population densities tend to an isolated periodic behavior, i.e., to a stable *limit cycle* which surrounds  $P_2$ . The limit cycle emerges from a *Hopf bifurcation*.

Figure 3 shows the phase portrait of the system (5).

### 3.3 The Spatiotemporal Model and Simulations

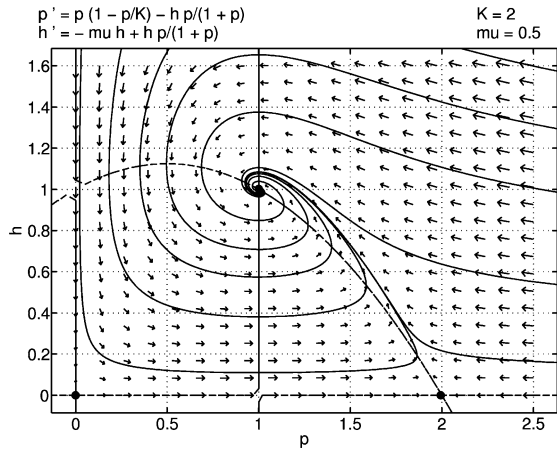
For the inclusion of the spatial variables, we assume: (1) The plants do not move but its population density changes in space because of the interaction with the herbivores, (2) The herbivores—at individual level—move at random and (3) The temporal dynamics of the interaction is described by the system (5). The resulting mathematical model is:

$$\begin{aligned} \frac{\partial p}{\partial t} &= p \left( 1 - \frac{p}{K} \right) - \frac{m_1 h p}{(s + p)}, \\ \frac{\partial h}{\partial t} &= D \Delta h + \frac{m_2 h p}{(s + p)} - \eta h, \end{aligned} \tag{6}$$

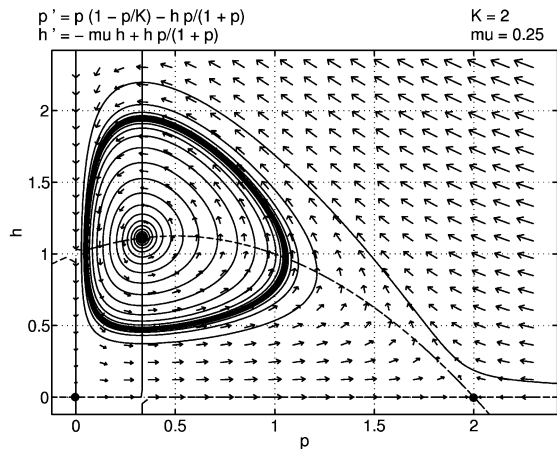
where  $K, m_1, s, D, m_2$ , and  $\eta$  are positive parameters. Here, the solution positiveness and boundedness of an initial and homogeneous Neumann boundary value problem associated with system (6) follows from the result appearing in Appendix B. For the numerical simulations, we take those parameter values for which the homogeneous system (5) has a limit cycle. Additionally, the initial conditions were a small spatial perturbation of the steady and homogeneous state of the system (6). These are

$$\begin{aligned} p(\vec{r}, 0) &= R(1 + 0.2 \sin(x + y) \cos(x - y)) \quad \text{and} \\ h(\vec{r}, 0) &= W(1 + 0.4 \sin(2x)), \quad \forall \vec{r} \in \mathcal{R}, \end{aligned}$$

**Fig. 3** Dynamics of the system (5) for  $\beta = 1$ ,  $K = 2$  and different values of  $\alpha$ . (b) shows the emergence of a limit cycle from a Hopf bifurcation. See the text



(a)  $\alpha = 1/2$ .



(b)  $\alpha = 1/4$ .

where  $R = 0.364$  and  $W = 1.11$  are about 10% perturbation of the homogeneous steady state. The numerics exhibit some interesting transients, including the fact that the herbivore population takes the qualitative initial distribution of the plants implying coexistence with the plants in the same parts of the habitat. But for big enough time, both population densities evolve toward spotted temporal periodic oscillations. The pulsating spots are aligned in rows. Therefore, for big enough time, at each fixed point of the rectangular habitat the local population densities change periodically in time as result of the Hopf bifurcation. This resembles to us the so-called *breathing patterns* which already have been reported in other contexts. For instance, in Muratov and Osipov (1996), the appearance of breathing (or pulsating) patterns in a type of activator-inhibitor system is discussed. Figure 4 shows our numerical simulations.

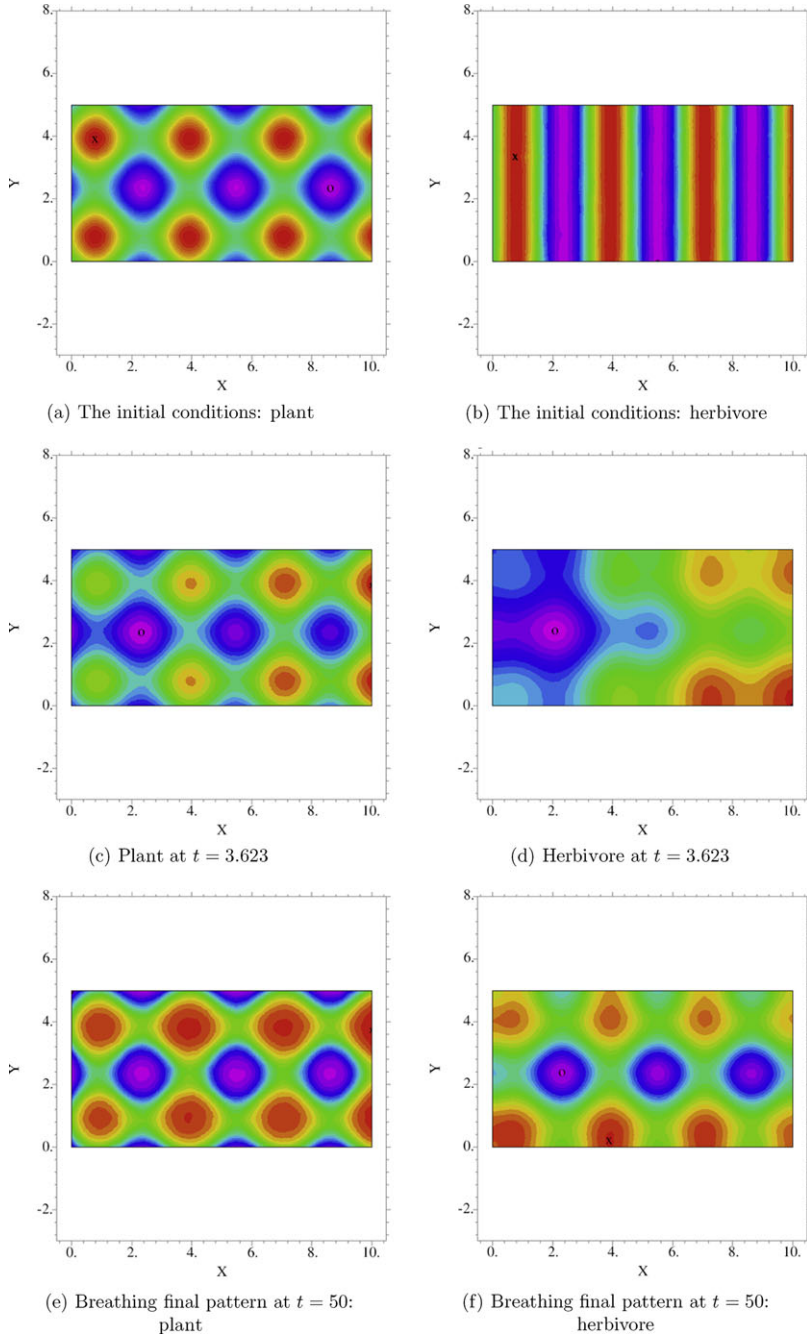


**Fig. 4** Numerical solutions of the system (6) for the parameter values  $D = 6$ ,  $K = 2$ ,  $m_1 = 1$ ,  $m_2 = 1$ ,  $s = 1$ , and  $\eta = 0.25$

## 4 The Pollinator–Plant–Herbivore Mathematical Model

In this section, we consider the full mathematical model for describing a pollinator–plant–herbivore interaction. Following the same scheme as in previous sections, we study the homogenous model first, and later on the nonhomogeneous one.

One important issue to being considered is the role played by a third species into the dynamics of a mutualistic interaction already kept by two populations. Hence, a herbivore species is added to the mutualistic interaction sustained by plants and pollinators.

### 4.1 The Assumptions and the Homogeneous Model

The hypothesis for the homogeneous model are: (1) The pollinators, in addition of having some benefits (nectar or pollen) from the plants, have other limited source of food, (2) The plants are pollinized exclusively by this pollinator population, (3) The pollinator–plant interaction is described by a Holling response of type II, (4) The plants are the unique food source for the herbivores, (5) The plant–herbivore interaction is described by a Holling response of type II, and (6) The herbivores interact with the pollinators indirectly: by reducing the pollinator visits rate to plants.

A mathematical model constructed on the above hypothesis is:

$$\begin{aligned} \dot{a} &= a \left( 1 - \frac{a}{K} \right) + \frac{g(h)k_2\sigma\mu ap}{1 + \sigma\phi\mu^2 p}, \\ \dot{p} &= -\gamma p + \frac{g(h)k_1\sigma\mu ap}{1 + \sigma\phi\mu^2 p} - \frac{m_1 ph}{s + p}, \\ \dot{h} &= -\delta h + \frac{m_2 ph}{s + p}, \end{aligned} \quad (7)$$

where  $g \in C^1[0, \infty)$ ,  $g(0) = 1$ ,  $g'(h) \leq 0$  and  $g(h) > 0 \forall h \geq 0$  is the *reduction rate of visits* of pollinators to plants which depends on the herbivore population density. All the parameters appearing in (7) are positive and have an important ecological interpretation. In fact,  $k_1$  is the number of fertilized ovums in each pollinator visit,  $\sigma$  is the probability of visits,  $\phi$  is a measure of the speed of nectar extraction, and  $\mu$  is the energetic recompense (see Jang 2002).

### 4.2 On the Temporal Dynamics

Because of the nonlinearity and the amount of parameters involved in the system (7)—as far as the authors knowledge, except a few results obtained by Jang (2002)—the dynamics of the system (7) is not completely known. Now, we are going to present a brief review of the results obtained by Jang. Later on, we present some of the numerical explorations we did.

For any parameter values, the points  $P_0 = (0, 0, 0)$  and  $P_1 = (K, 0, 0)$  are equilibria of the system (7). The nontrivial branch of the null-clines of (7) are

$$f_1 \equiv \left( 1 - \frac{a}{K} \right) + \frac{g(h)k_2\sigma\mu p}{1 + \sigma\phi\mu^2 p} = 0, \quad f_2 \equiv -\gamma + \frac{g(h)k_1\sigma\mu a}{1 + \sigma\phi\mu^2 p} - \frac{m_1 h}{s + p} = 0,$$

and

$$f_3 \equiv -\delta + \frac{m_2 p}{s + p} = 0.$$

An extreme case.  $g(h) \equiv 1$ . Here, whenever  $m_2 > \delta$ , there exists a nontrivial equilibrium for (7):  $\bar{P} = (\bar{a}, \bar{p}, \bar{h})$  where

$$\begin{aligned} \bar{a} &= K \left[ 1 + \frac{k_2 \mu \sigma \bar{p}}{1 + \phi \sigma \mu^2 \bar{p}} \right], & \bar{p} &= \frac{s \delta}{m_2 - \delta} \quad \text{and} \\ \bar{h} &= \frac{(s + \bar{p})}{m_1} \left[ -\gamma + \frac{k_1 \mu \sigma \bar{a}}{1 + \sigma \phi \mu^2 \bar{p}} \right]. \end{aligned}$$

In the following points, we summarize the local phase space of the system (7):

1.  $P_0$  is a saddle point for all parameter values. The two-dimensional stable manifold lies in the  $ph$  plane. Therefore, if there is a pollinator population and the plant and herbivore populations are small enough, both species become extinct;
2.  $P_1$ ,
  - is a local attractor if  $\mu < \gamma/k_1\sigma$ . Hence, if the population densities of the three species are in a small neighborhood of  $P_1$ , the trajectories of (7) tend to this point,
  - is a saddle point if  $\mu > \gamma/k_1\sigma$  whose two-dimensional stable manifold is in the  $ah$  plane. Therefore, for small enough population densities, plants and herbivores become extinct and the pollinators population stabilizes at  $K$ .
3. Given appropriate parameter values, the point  $\bar{P}$  is locally asymptotically stable.

On the global analysis. Let us introduce the following definition.

**Definition 4.1** The system  $\dot{x} = F(x)$  is called *persistent*, if  $\lim_{t \rightarrow \infty} x_i(t) > 0$  where  $x(t) = (x_i(t))_{1 \leq i \leq n}$  is any solution with  $x_i(0) > 0$  for  $1 \leq i \leq n$ . The system is *uniformly persistent*, if there exists  $d > 0$  such that  $\lim_{t \rightarrow \infty} x_i(t) \geq d$  for  $1 \leq i \leq n$  and for any solution with positive initial conditions.

The following theorem summarizes Jang’s results.

**Theorem 4.1** (Cited from Jang 2002)

1. The solutions of the system (7) starting from  $(a_0, p_0, h_0)$  with  $a_0, p_0$ , and  $h_0$  greater or equal zero, are not negative and bounded for all  $t$ ,
2. Let  $\mu > \mu_1$ , then the system (7) is uniformly persist if  $h(\bar{p}^*) > \delta/m_2$ ,
3. All solution of the system with  $a(0) > 0$  and  $p(0) > 0$  converges to  $(\bar{a}^*, \bar{p}^*, 0)$  if  $h(\bar{p}^*) < \delta/m_2$ .

A particular case. Here, we consider the system (7) by choosing the particular form for the reduction rate of visits:

$$g(h) = \frac{1}{1 + k_3 h^2}, \quad \text{with } k_3 > 0,$$

which has the qualitative behavior mentioned previously. In this case, the existence of a positive unique equilibrium,  $(a^*, p^*, h^*)$  is possible to prove for system (7). See the Appendix A. Thus, on the basis of its existence, we carried out a set of numerical simulations.<sup>6</sup> These allow us to see a rich dynamics supported by the system (7), including:

- The existence of a homoclinic trajectory based at the equilibrium  $P = (K, 0, 0)$  for a small enough value of  $K$ . Meanwhile, for bigger values of  $K$ , the homoclinic loop breaks leading to other dynamical behaviors,
- The emergence of a stable limit cycle implies that the three populations remains; that is, each population density tends to a time periodic function for a long enough time.
- The existence of a global attractor. In this case, the populations persist and their respective densities tend to a constant value as the time goes to infinity.

These behaviors were obtained by increasing the values of  $K$ . Figure 5 contains some phase portraits of (7) for several  $K$  values.

### 4.3 On the Spatiotemporal Dynamics

For the derivation of the mathematical model, we consider the following assumptions: (1) The pollinators movement has two components: its “own” at random individual movement and a drift (advection) due to, for instance, the wind. Here, we are going to consider a constant advection velocity,  $\vec{v}$ , (2) At individual level, the herbivores also move at random and their movement is supposed much slower than that of the pollinators, (3) The spatial distribution of the plants changes because the interaction with the pollinator and herbivore populations, and (4) The population interactions are described by the system (7). A model which captures these assumptions is given by:

$$\begin{aligned} \frac{\partial a}{\partial t} &= D_1 \Delta a - \vec{v} \cdot \nabla a + a \left( 1 - \frac{a}{K} \right) + \frac{g(h)k_2 \sigma \mu a p}{1 + \sigma \phi \mu^2 p}, \\ \frac{\partial p}{\partial t} &= -\gamma p + \frac{g(h)k_1 \sigma \mu a p}{1 + \sigma \phi \mu^2 p} - \frac{m_1 p h}{s + p}, \\ \frac{\partial h}{\partial t} &= D_2 \Delta h - \delta h + \frac{m_2 p h}{s + p}, \end{aligned} \tag{8}$$

for all  $(x, y) \in \mathcal{R}$  defined previously and  $t > 0$ .

Determine and classify existence of possible ordered spatial structures (patterns) associated with the problem (8) corresponding to different set of feasible parameter values and initial and boundary value conditions is an important challenge even from an interpretative point of view. As far the authors knowledge, this problem is not solved yet. What we present here are just some preliminary results which come from the numerical simulations we have performed. For this purpose, we used the parameter values for which the temporal dynamics suggests the existence of a globally

<sup>6</sup>All the three-dimensional space phases contained in this paper were done by using the *ODE45 MATLAB*, version 7.0 routine.

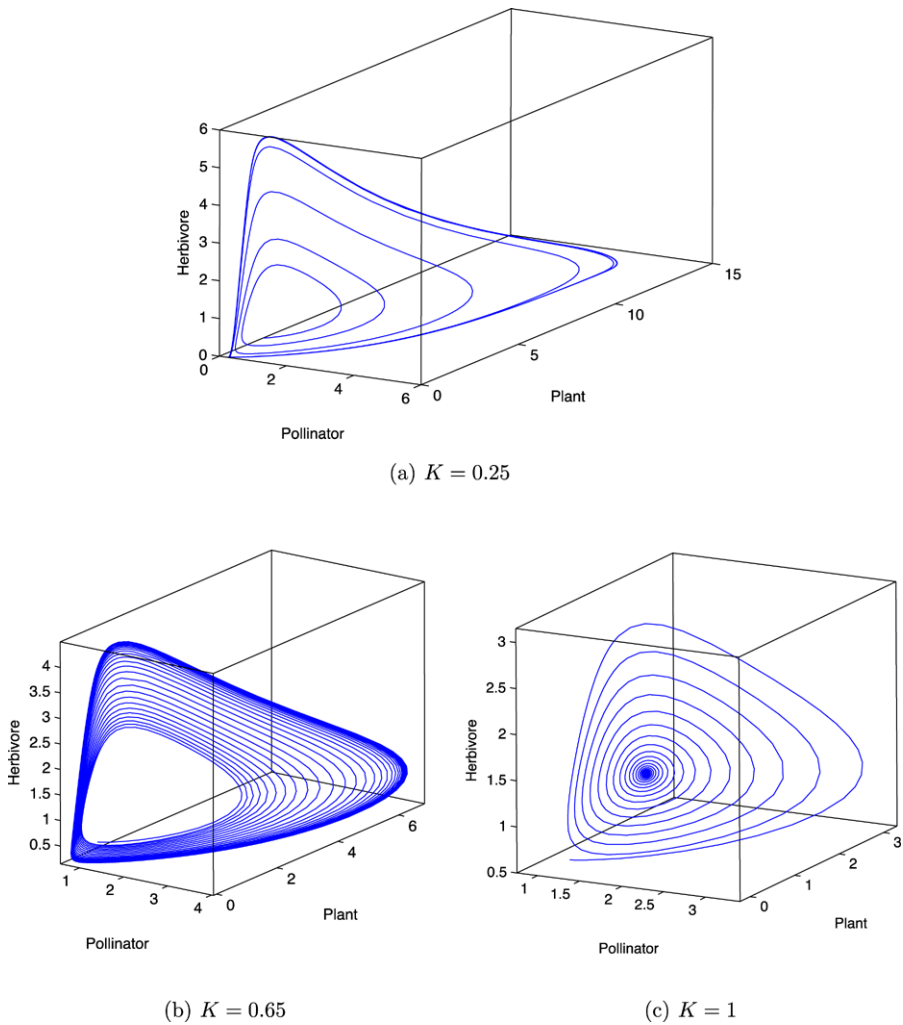


**Fig. 5** Phase portrait of the system (7) corresponding to different parameter values

asymptotically stable equilibrium. The initial conditions along the rest of the paper are:

$$a(\vec{r}, 0) = U(1 + 0.9 \sin(2y)), \quad p(\vec{r}, 0) = W(1 + 0.9 \sin(2x)),$$

and

$$h(\vec{r}, 0) = R(1 + 0.9 \sin(x + y) \cos(x - y)),$$

where  $(U, W, R) = (0.25, 0.01, 0.01)$ . Note that the initial conditions we selected, correspond to a spatial perturbation of the homogeneous state which our numerical simulations exhibit it as a global attractor.

Nevertheless, for our particular problem, we have done this analysis using comparison techniques based on the concepts of sub and supersolutions. In Appendix B, we present an overview of the proofs, and in Sánchez-Garduño and Breña-Medina (2010) the reader will find full technical details.

In order to see the separate effect of the diffusion and the advection terms into the final spatial distributions of the populations described by (8) on the region on  $\mathcal{R}$ , we consider each separate process by taking into account two types of homogeneous boundary conditions: Dirichlet and Neumann.

#### 4.3.1 Numerical Simulations of the Reaction–Diffusion Model

Here, we consider the system (8) with  $\vec{v} = (0, 0)$ ,  $D_1 = 3$ ,  $D_2 = D_1/10$ , and for each boundary condition mentioned above.

The homogeneous Dirichlet boundary condition corresponds to the case where no individuals of any population is present on  $\partial\mathcal{R}$  for all  $t$ . Figures 6 and 7 show the result of our numerical simulations. Those show: the initial, some transients, and the final population distributions, respectively. As can be seen in above mentioned figures, is a remarkable increasing of the plant population in the central part of the region  $\mathcal{R}$  originating a migratory movement of the pollinator and herbivore populations toward the same area. Moreover, after a very long time ( $10^4$  iterations), the ecological coexistence of the three populations, is observed and they do so in such a way that no significant difference between a transient spatial distribution and the final distributions of the populations are observed. Even though a set of different initial conditions were considered, the result of the numerics in all cases showed no substantial differences in the final distribution of the populations.

The homogeneous Neumann boundary condition corresponds to the case where there is not flux of the populations on  $\partial\mathcal{R}$  for all  $t$ . By considering the same parameter values as in the previous case, an interesting phenomenon is shown. As a matter of fact, the population density distributions evolve in such way that pollinators population moves toward places where the plant population density is higher; in other words, an aggregation phenomena seems to appear. This originates a slow herbivore population movement toward the same region, as though they were chasing pollinators. As result of this, the plant population dramatically decreases in these areas. Nevertheless, in those regions where the presence of herbivores is less the plant population density increases as had been suspected, which stimulates a pollinator movement to the same areas which, consequently, originates a herbivores displacement. Hence, a periodical traveling wave-like dynamic from left to right for each population density can be observed. See Figs. 8 and 9.

#### 4.3.2 Numerical Simulations of the Reaction–Diffusion–Advection Model

As previously, system (8) with  $\vec{v} = (v, 0)$ ,  $D_1 = 3$ ,  $D_2 = D_1/10$ , and  $v = 3$ , for each boundary condition mentioned above, we consider the same initial conditions (Figs. 10(a), 10(c), and 10(e)). In addition, ought to transport term, determined by the vector  $\vec{v} = (v, 0)$ ,—in addition to its “natural” random movement—there is a drift in the movement of the pollinators population which points vector  $\vec{v}$  out.

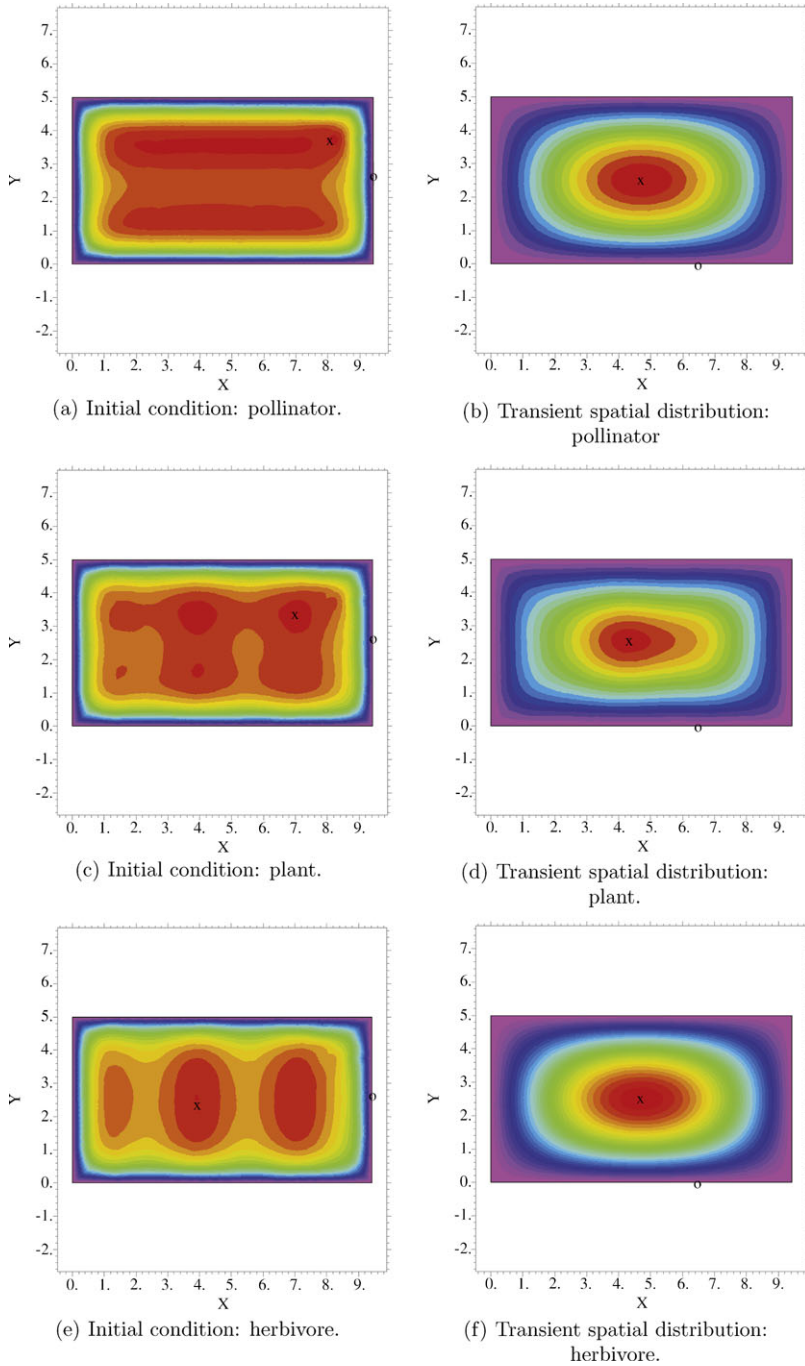


**Fig. 6** Numerical solutions of an initial and homogeneous Dirichlet boundary values problem associated with the RD system (8) at different snapshots

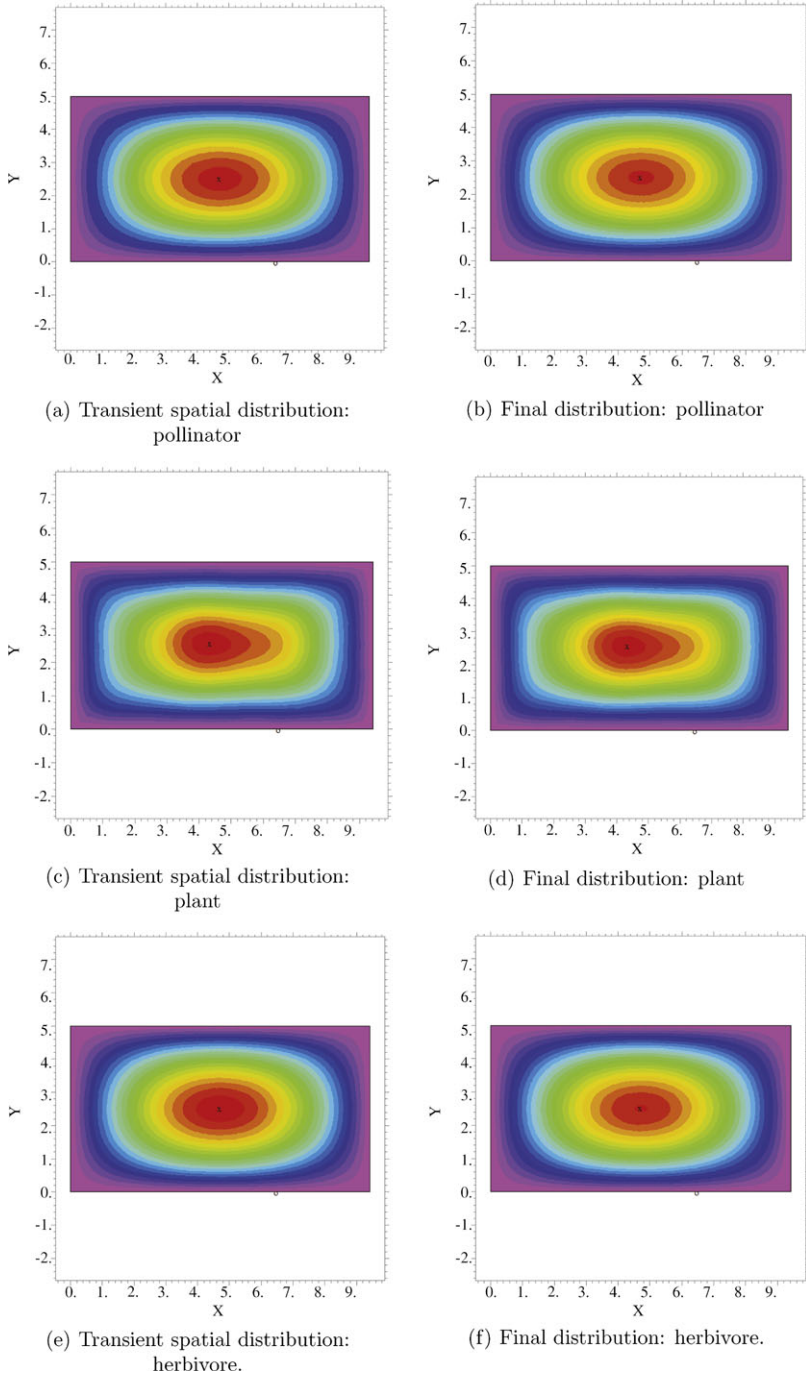


**Fig. 7** Numerical solutions of an initial and homogeneous Dirichlet boundary values problem associated with the RD system (8) at different snapshots

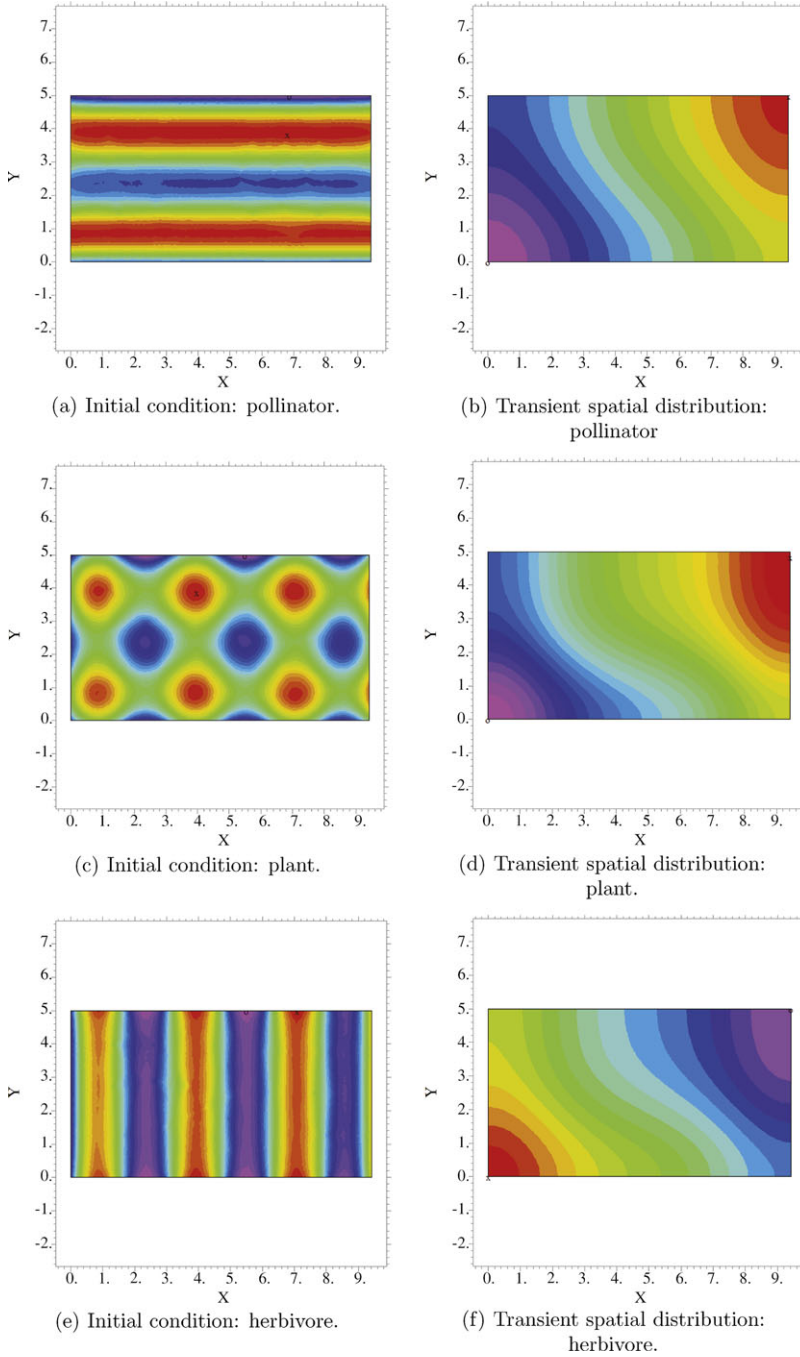


**Fig. 8** Numerical solutions of an initial and homogeneous Neumann boundary values problem associated with the RD system (8) at different snapshots

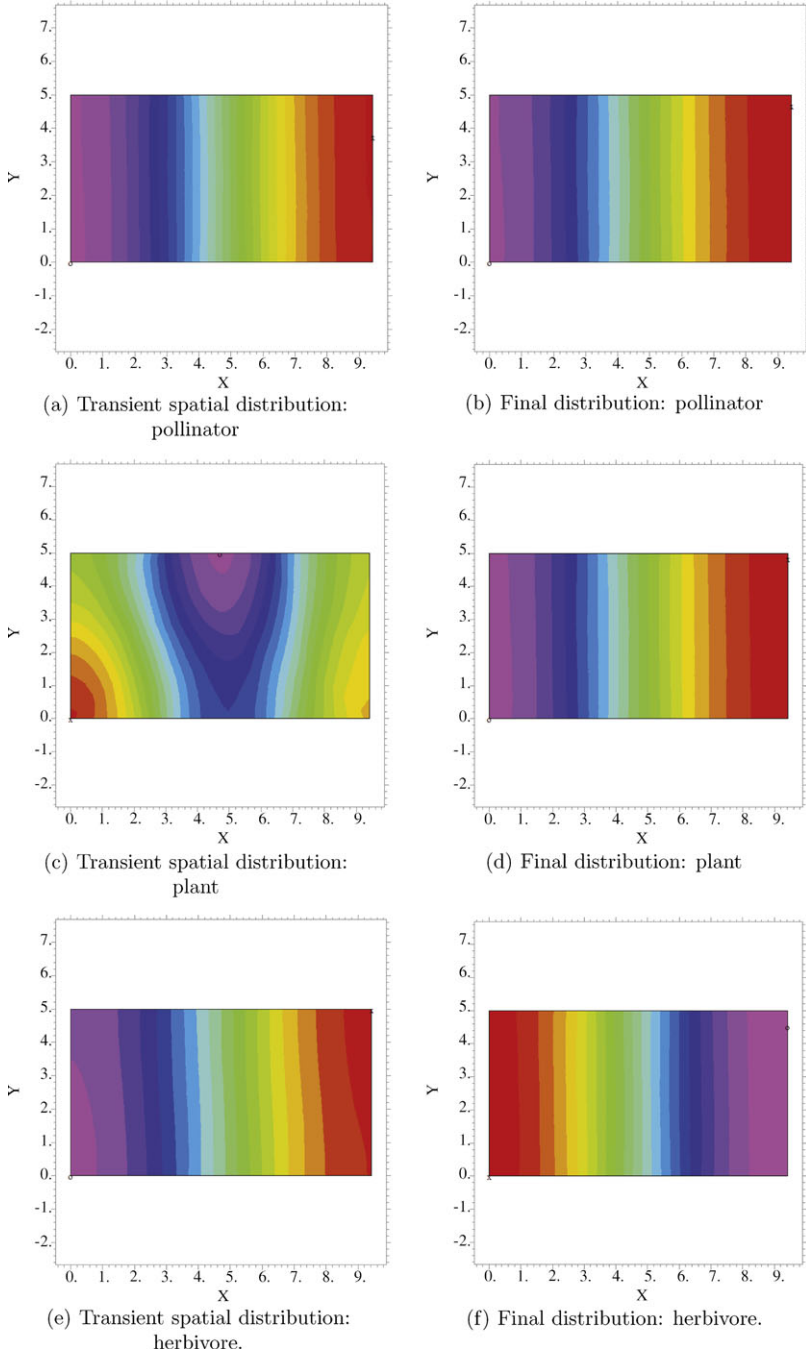


**Fig. 9** Numerical solutions of an initial and homogeneous Neumann boundary values problem associated with the RD system (8) at different snapshots

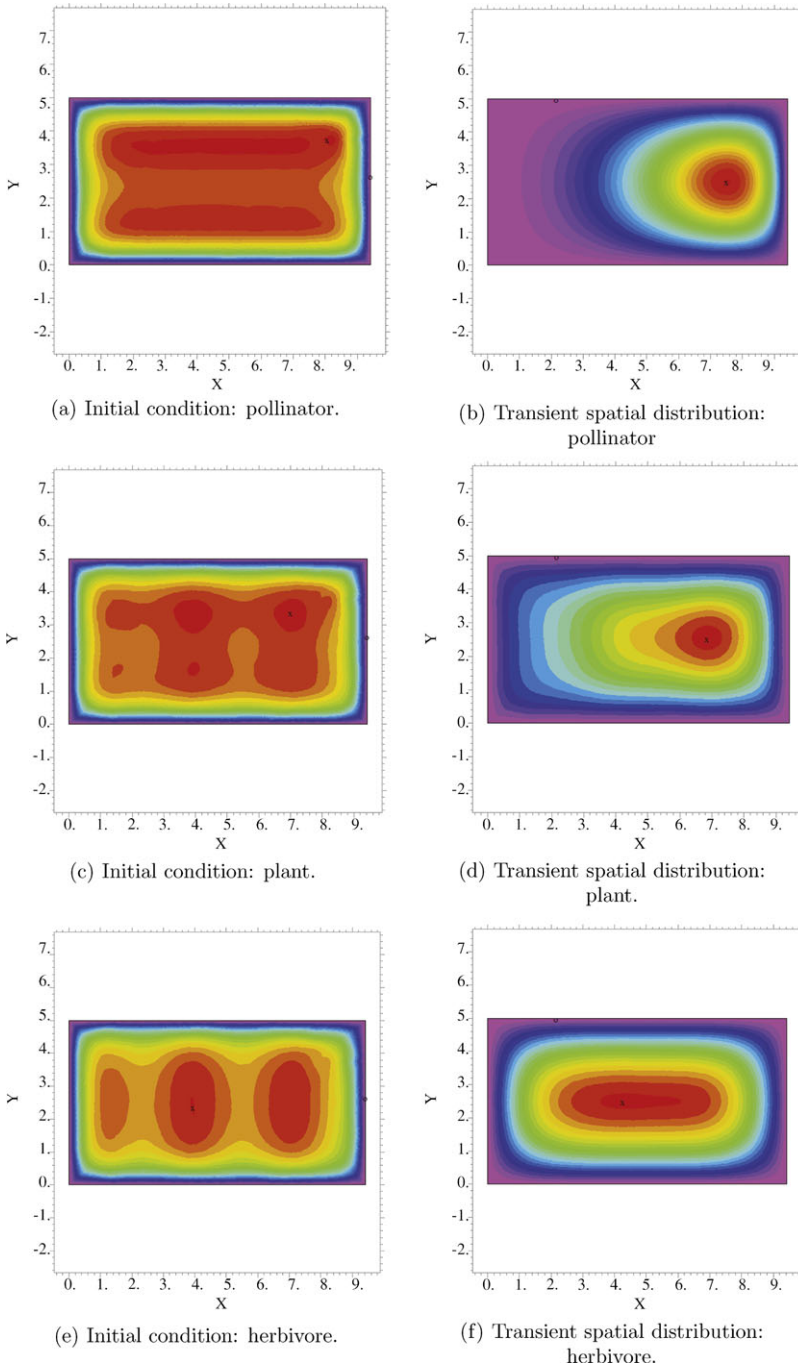


**Fig. 10** Numerical solutions of an initial and homogeneous Dirichlet boundary values problem associated with the RDA system (8) with  $\vec{v} = (v, 0)$  at different snapshots

For our first set of numerical simulations, homogeneous Dirichlet boundary conditions are considered. Results can be seen in the Figs. 10 and 11 which show the spatial distribution of the three populations at different running times, namely the initial, an intermediate, and big enough, respectively. As a matter of fact, not only interesting transient distributions are observed but also the final ones. As a consequence of the advection term and boundary conditions, the pollinator population is driven to the domain's right side, however, the three populations tend to localize in the domain core.

Now, let us consider homogeneous Neumann boundary conditions. The initial, transient, and final distributions—as result of our numerical simulations—can be seen in Figs. 12 and 13. They show some final spatial pattern features which, in fact, have some similitude with the no-advection case. These take the form of traveling wave-like patterns for the three population densities. However, a different transient dynamic is exhibited as well. Indeed, as can be seen in Figs. 12(b), 12(d), and 12(f), these waves start with a high density region localized in the lower left corner of  $\mathcal{R}$  and smoothly travel from left to right side of the rectangle. Additionally, the plant population density traveling wave moves quicker than the others, then is followed by the pollinator and herbivore population waves. This specific traveling wave behavior was expected because the drift produced by the transport term on the gradient of the pollinator population point out horizontally from left to right, as for  $-\vec{v} \cdot \nabla a$  provides this flow. However, a periodical traveling wave is seen in a similar fashion as that in the nonadvection term case. See Fig. 13.

Moreover, additional numerical simulations were carried out by using different constant vectors  $\vec{v}$ . In all cases, the same qualitative behavior described previously was observed.

## 5 Conclusions and Discussion

In this final section, we recapitulate our findings. Also, some problems which we consider it is worth to investigate in this field are listed.

1. The specific numerical simulations we performed on the full pollinator-plant-herbivore mathematical model show that the spatial distribution of the populations over the habitat during the running time of the software FlexPDE, strongly depends upon the competition between the diffusion (in the pollinators and herbivores) and advection processes in the pollinators. The dominance of one process or another, depends on the selected value of  $D_1$ ,  $D_2$  and the magnitude of the advective velocity  $\vec{v}$ .
2. The homogeneous boundary conditions play an important role in the spatial distribution of the populations. In fact, the homogeneous Dirichlet conditions force the three populations to abandon the borders initiating a migratory movement toward the central part of the region  $\mathcal{R}$ ; meanwhile the homogeneous Neumann conditions allow the populations to survive over  $\mathcal{R}$  exhibiting different heterogeneous distribution patterns. Nonetheless, a theoretical study is required.
3. In this paper, the Holling response of type II was abundantly used. However, the so-called Holling response of type IV has been extensively documented in the

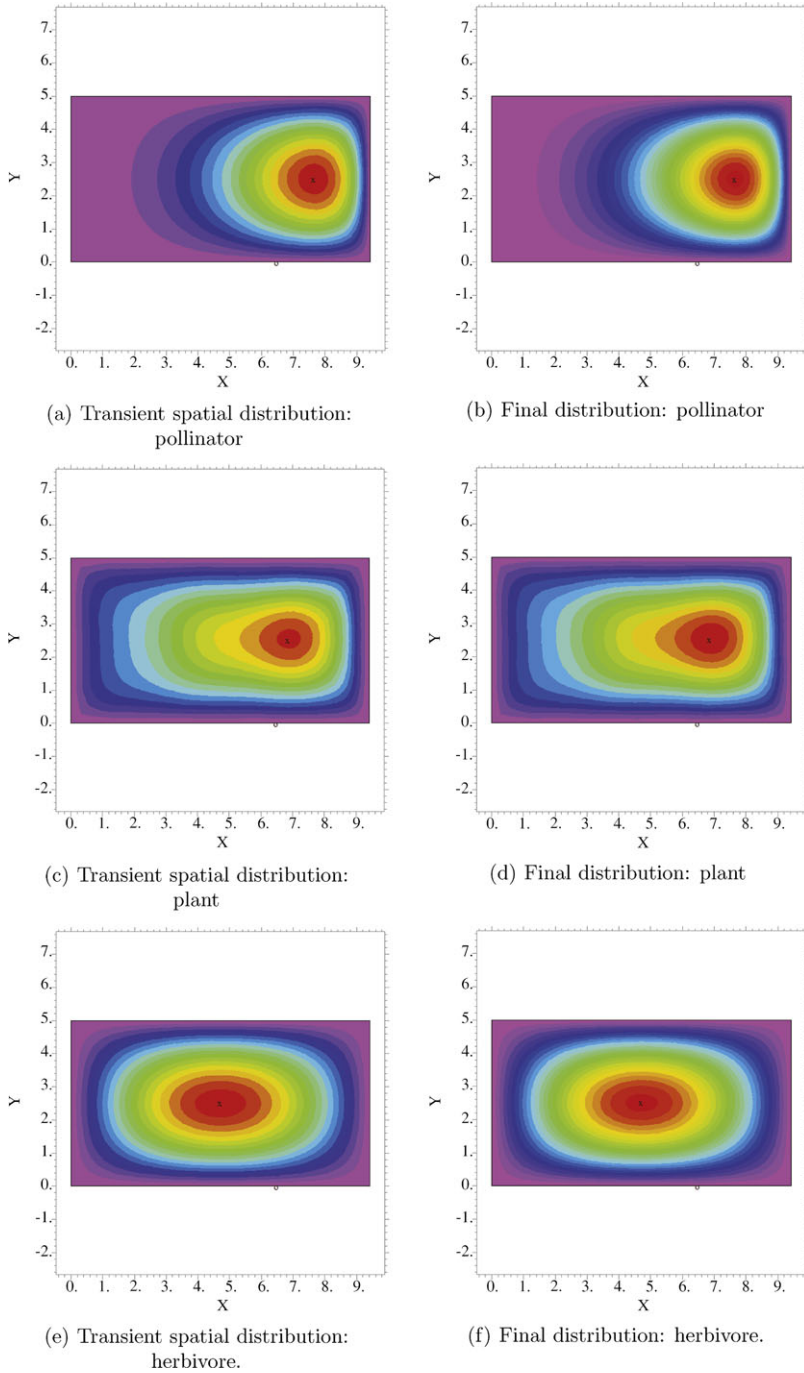


**Fig. 11** Numerical solutions of an initial and homogeneous Dirichlet boundary values problem associated with the RDA system (8) with  $\vec{v} = (v, 0)$  at different snapshots

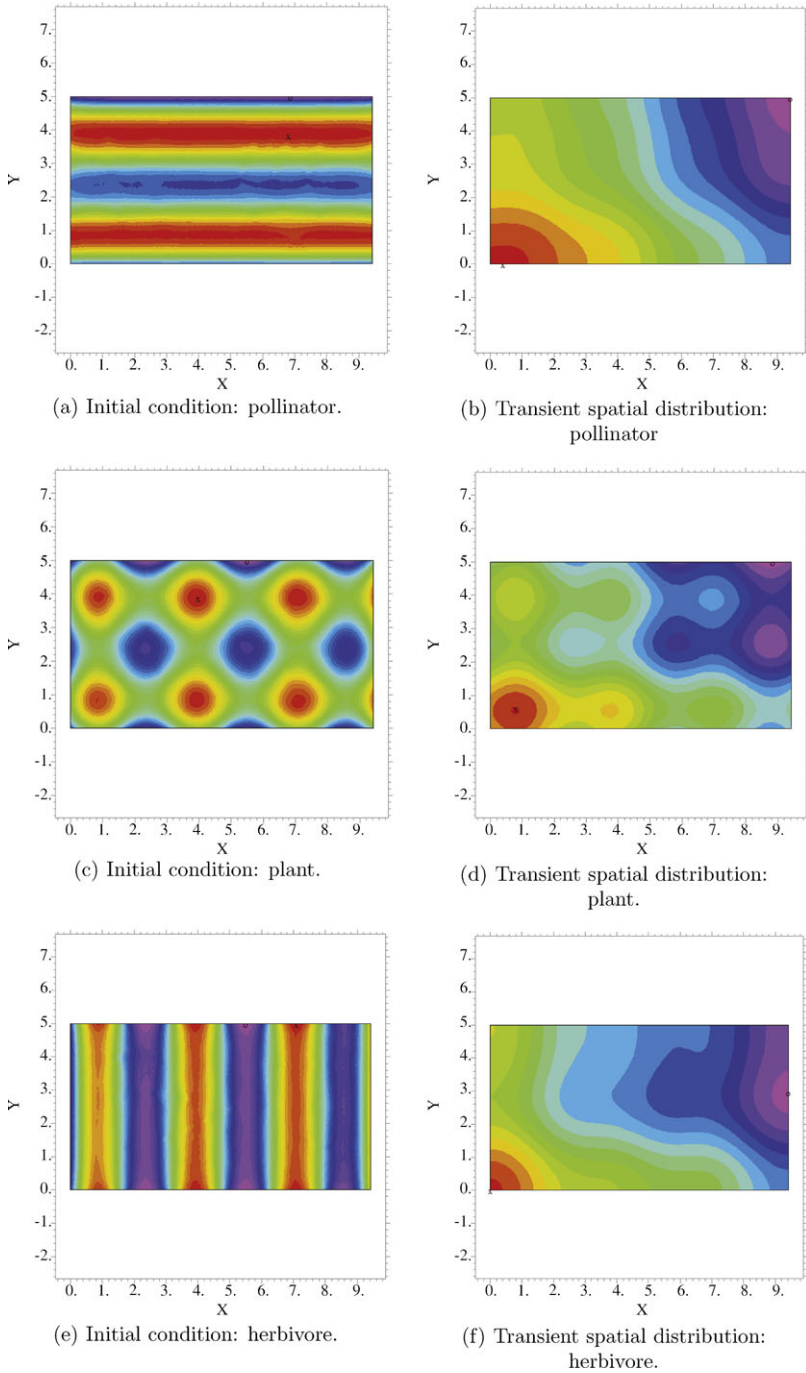


**Fig. 12** Numerical solutions of an initial and homogeneous Neumann boundary values problem associated with the RDA system (8) with  $\vec{v} = (v, 0)$  at different snapshots

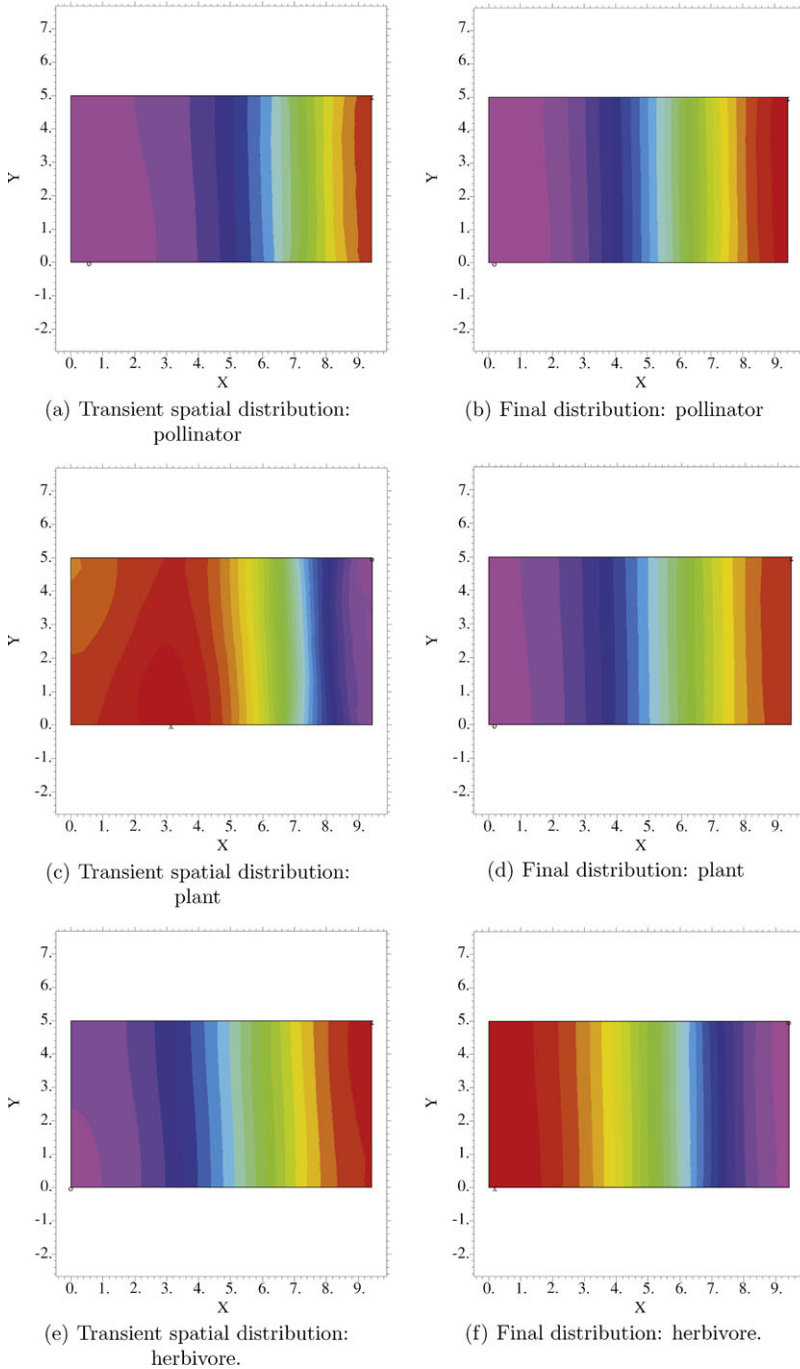


**Fig. 13** Numerical solutions of an initial and homogeneous Neumann boundary values problem associated with the RDA system (8) with  $\vec{v} = (v, 0)$  at different snapshots

ecological literature (see Collings 1997 and Crawley 1992). According which, the predation rate per predator is a monotone increasing function for small enough prey density values becoming a monotone decreasing function for larger prey density values. The incorporation of this type of functional response into the herbivore-plant interaction should result in an interesting problem. This is currently studied by one of us and his students (see Quilantán 2010 and Velázquez 2008).

4. Some theoretical problems associated with the RDA system presented here remain to be solved. These include a detailed local and global bifurcation analysis for the homogeneous pollinator-plant-herbivore mathematical model. Also, an analysis with the aim of predicting the possible spatial patterns of the model, is required.
5. In a more realistic situation, the pollinator and herbivore movement should be toward those places of the habitat where the population density of plants is high. In such a case, instead of having constant diffusion coefficients in the pollinator and herbivore equations, those should be plant population, and even spatial and temporal dependent. Indeed, the incorporation of this factor—in addition to being an important theoretical problem—also has relevance in interpretative terms.

**Acknowledgements** FSG thanks the *División Académica de Ciencias Básicas de la Universidad Juárez Autónoma de Tabasco (UJAT)* for the hospitality and facilities provided to him during a sabbatical semester he spent there.

### Appendix A: The Existence of a Positive Equilibrium

In this Appendix, the existence of a positive equilibrium for the system (7) is shown, where  $g(h) = 1/(1 + k_3h^2)$ . For this aim, let us simplify the notation in (7) by introducing  $\beta$ ,  $\alpha_1$ , and  $\alpha_2$  as follows:  $\beta = \sigma\phi\mu^2$ ,  $\alpha_1 = k_2\sigma\mu$  and  $\alpha_2 = k_1\sigma\mu$ .

Setting the herbivore field in (7) equal zero, we obtain  $p = p^* = s\delta/(m_2 - \delta)$ , where the condition  $m_2 > \delta$  is required in order to guarantee  $p > 0$ , which in the phase space—for each positive  $p$ —defines a plane parallel to the plane  $ap$ . Then in order to seek equilibrium points, we search them on the null-clines projections onto the plane  $p \equiv p^*$ . That is, given a fixed  $p^*$  value, the equation  $f_1 = 0$  implies

$$g(h^*) = \frac{(a^* - K)(1 + \beta p^*)}{K\alpha_1 p^*}, \tag{A.1}$$

where  $a^* > K$ . Now, by writing down the explicit form of  $g$  in (A.1), we find a first relationship between  $h^*$  and  $a^*$ ,

$$h_1^*(a^*) = \sqrt{\frac{K\alpha_1 p^* - (a^* - K)(1 + \beta p^*)}{k_3(a^* - K)(1 + \beta p^*)}}, \tag{A.2}$$

which defines a positive function for  $h_1^*$ , whenever  $a^*$  satisfies the inequality

$$K < a^* < \left[ \frac{1 + (\alpha_1 + \beta) p^*}{1 + \beta p^*} \right] K.$$

On the other hand, another relationship for  $h^*$  and  $a^*$  is obtained from the equality  $f_2 = 0$ , namely

$$h_2^*(a^*) = \frac{(s + p^*)}{m_1} \left[ \frac{\alpha_2}{K \alpha_1 p^*} (a^* - K) a^* - \gamma \right], \tag{A.3}$$

which defining  $a_c^*$  as

$$a_c^* := \frac{K}{2} + \frac{1}{2} \sqrt{K^2 + \frac{4\gamma K \alpha_1 p^*}{\alpha_2}},$$

guaranties positive values for  $h_2^*$  for all  $a^* > a_c^*$ . Due to this fact, (A.2) is a real function and  $a_c^* > K$ , inequalities

$$a_c^* < a^* < \left[ \frac{1 + (\alpha_1 + \beta) p^*}{1 + \beta p^*} \right] K, \tag{A.4}$$

with

$$K > \frac{\alpha_1 \gamma (1 + \beta p^*)^2 p^*}{\alpha_2 (1 + (\alpha_1 + \beta) p^*) (2 + (\alpha_1 + 2\beta) p^*)}, \tag{A.5}$$

must be held in order to assure positiveness for  $h_1^*$  and  $h_2^*$  on the interval where  $a^*$  varies.

Therefore, once given fixed  $p^*$  values,  $a^*$  and  $h^*$  must satisfy (A.2) and (A.3). Figure 14 shows the behavior of  $h_1^*$  and  $h_2^*$  as a function of  $a^*$  for different values of parameter  $K$ . As it can be seen, for each  $K$ —and appropriate parameter values given by  $m_2 > \delta$ , (A.4), and (A.5)—those graphs meet only in exactly one point belonging to the first quadrant. In consequence, system (7) has exactly one equilibrium point in the first positive octant, as is claimed.

### Appendix B: Existence, Positiveness and Boundedness

Given a mathematical problem, searching the existence and uniqueness of solution for it is a quite important, mathematical and interpretative points of view, objective. In our case, because of the ecological interpretation of the model variables, we should guarantee positiveness and boundedness of the solution of the initial and boundary value problem. This Appendix deals with them. A schematic and qualitative description of results—a complete report, can be seen in Sánchez-Garduño and Breña-Medina (2010)—is presented. Comparison techniques approach, where the concepts of quasimonotone vector fields, sub and supersolutions of parabolic systems, is used.

The following initial and boundary condition problem is examined:

$$\begin{aligned} \frac{\partial a}{\partial t} &= D_1 \Delta a - \vec{v} \cdot \nabla a + a \left( 1 - \frac{a}{K} \right) + \frac{g(h)k_2 \sigma \mu a p}{1 + \sigma \phi \mu^2 p}, \\ \frac{\partial p}{\partial t} &= -\gamma p + \frac{g(h)k_1 \sigma \mu a p}{1 + \sigma \phi \mu^2 p} - \frac{m_1 p h}{s + p}, \end{aligned} \tag{B.1}$$

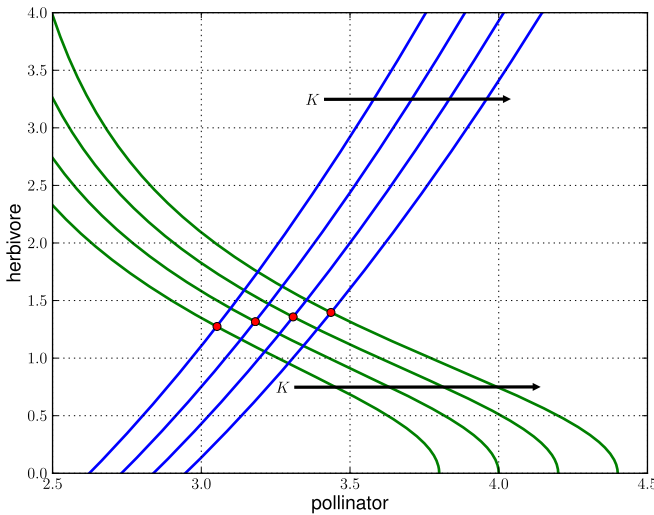


**Fig. 14** Graphical representation of the positive equilibrium point—dots—given by (A.2) and (A.3)—decreasing and increasing curves, respectively—for soaring values of parameter  $K$ . They lay on the plane  $p = p^*$  for positive  $a$  and  $h$ . See the text for details

$$\frac{\partial h}{\partial t} = D_2 \Delta h - \delta h + \frac{m_2 p h}{s + p},$$

for all  $(x, y) \in \mathcal{R}$  and  $t > 0$ , with homogeneous Neumann boundary conditions on  $\partial R$ . In order to simplify system (8) notation,  $c_1, c_2$ , and  $c_3$  are introduced as follows:  $c_1 = k_2 \sigma \varphi \mu$ ,  $c_2 = \varphi \sigma \mu^2$ , and  $c_3 = k_1 \sigma \varphi \mu$ . Now, we define the vector field  $\vec{F} : \mathbb{R}^3 \rightarrow \mathbb{R}^3$  whose components are:

$$F_1(a, p, h) = a \left( 1 - \frac{a}{K} \right) + g(h) \frac{c_1 a p}{1 + c_2 p},$$

$$F_2(a, p, h) = -\gamma p - \frac{m_2 p h}{s + p} + g(h) \frac{c_3 a p}{1 + c_2 p}$$

and

$$F_3(p, h) = -\eta h + \frac{m_1 p h}{s + p}.$$

It can be seen that the nonlinear functions  $F_j$  with  $j = 1, 2, 3$ , belong to the set  $C^1_{\mathbb{R}^3_+}$ , and consequently, they have bounded first partial derivatives on  $\mathbb{R}^3_+$ . They also are  $\alpha$ -Holder continuous functions of order one. Observe that, for all greater or equal zero values of  $a, p$ , and  $h$ , the following inequalities hold:

$$\frac{\partial F_1}{\partial p} \geq 0, \quad \frac{\partial F_1}{\partial h} \leq 0, \quad \frac{\partial F_2}{\partial a} \geq 0, \quad \frac{\partial F_2}{\partial h} \leq 0,$$

$$\frac{\partial F_3}{\partial p} \geq 0, \quad \text{and} \quad \frac{\partial F_3}{\partial a} = 0,$$

hence, the vector field  $\vec{F}$ , having components  $F_j$ , is quasimonotone<sup>7</sup> on the  $\mathbb{R}^3$  first octant.

Now, let us denote by  $\hat{u} = (\hat{a}, \hat{p}, \hat{h})$  and  $\check{u} = (\check{a}, \check{p}, \check{h})$  the *supersolutions* and *subsolutions*, respectively. These are such that  $\hat{u} \geq \check{u}$  for all  $(\vec{x}, t) \in \mathcal{R}$ . By definition,  $\hat{u}$  and  $\check{u}$  must satisfy the following initial and boundary value problems, which are expressed in terms of differential inequalities (see Pao 1992, Chap. 8, Sect. 8.8 for details):

$$\begin{aligned} \frac{\partial \hat{a}}{\partial t} - D_1 \Delta \hat{a} + \vec{v} \cdot \nabla \hat{a} &\geq \hat{a} \left( 1 - \frac{\hat{a}}{K} \right) + g(\check{h}) \frac{c_1 \hat{a} \hat{p}}{1 + c_2 \hat{p}}, \\ \frac{\partial \hat{p}}{\partial t} &\geq -\gamma \hat{p} - \frac{m_2 \hat{p} \check{h}}{s + \hat{p}} + g(\check{h}) \frac{c_3 \hat{a} \hat{p}}{1 + c_2 \hat{p}}, \\ \frac{\partial \hat{h}}{\partial t} - D_2 \Delta \hat{h} &\geq -\eta \hat{h} + \frac{m_1 \hat{p} \hat{h}}{s + \hat{p}}. \end{aligned} \tag{B.2}$$

and

$$\begin{aligned} \frac{\partial \check{a}}{\partial t} - D_1 \Delta \check{a} + \vec{v} \cdot \nabla \check{a} &\leq \check{a} \left( 1 - \frac{\check{a}}{K} \right) + g(\hat{h}) \frac{c_1 \check{a} \check{p}}{1 + c_2 \check{p}}, \\ \frac{\partial \check{p}}{\partial t} &\leq -\gamma \check{p} - \frac{m_2 \check{p} \hat{h}}{s + \check{p}} + g(\hat{h}) \frac{c_3 \check{a} \check{p}}{1 + c_2 \check{p}}, \\ \frac{\partial \check{h}}{\partial t} - D_2 \Delta \check{h} &\leq -\eta \check{h} + \frac{m_1 \check{p} \check{h}}{s + \check{p}}, \end{aligned} \tag{B.3}$$

with the initial conditions:

$$\begin{aligned} \hat{a}(0, \vec{x}) &\geq a_0(\vec{x}) \geq \check{a}(0, \vec{x}); & \hat{p}(0, \vec{x}) &\geq p_0(\vec{x}) \geq \check{p}(0, \vec{x}); \\ \hat{h}(0, \vec{x}) &\geq h_0(\vec{x}) \geq \check{h}(0, \vec{x}) \end{aligned}$$

and boundary conditions:

$$\frac{\partial \hat{a}}{\partial n} \geq 0 \geq \frac{\partial \check{a}}{\partial n}; \quad \frac{\partial \hat{p}}{\partial n} \geq 0 \geq \frac{\partial \check{p}}{\partial n}; \quad \frac{\partial \hat{h}}{\partial n} \geq 0 \geq \frac{\partial \check{h}}{\partial n},$$

where  $\partial(\cdot)/\partial n \equiv \nabla(\cdot) \cdot \vec{n}$ , and  $\vec{n}$  is the outer normal vector on  $\partial \mathcal{R}$ .

With the aim of finding  $\hat{u}$  and  $\check{u}$ , let  $(\tilde{A}, \tilde{P}, \tilde{H})$  be the solution of the initial and boundary values problem

$$\begin{aligned} \frac{\partial A}{\partial t} - D_1 \Delta A + \vec{v} \cdot \nabla A &= A \left( 1 - \frac{A}{K} \right), \\ \frac{\partial P}{\partial t} &= -\gamma P - m_2 H, \end{aligned} \tag{B.4}$$

<sup>7</sup>This happens whenever the sign of  $\partial F_j / \partial x_i$  is different for  $i \neq j$ , where  $x_1 = a, x_2 = p$  and  $x_3 = h$ .

$$\frac{\partial H}{\partial t} - D_2 \Delta H = (-\eta + m_1)H,$$

with boundary conditions

$$\frac{\partial A}{\partial n} = 0, \quad \frac{\partial P}{\partial n} = 0, \quad \text{and} \quad \frac{\partial H}{\partial n} = 0, \quad \text{on } \partial \mathcal{R}$$

and positive initial conditions

$$A(0, \vec{x}) = a_0(\vec{x}); \quad P(0, \vec{x}) = p_0(\vec{x}); \quad H(0, \vec{x}) = h_0(\vec{x}) \quad \forall \vec{x} \in \mathcal{R}.$$

We can prove the following proposition.

**Proposition B.1** *There exist  $k_*$  and positive constants  $\rho_1$  and  $\rho_2$  such that the components  $\tilde{P}$  and  $\tilde{H}$  of the solution,  $(\tilde{A}, \tilde{P}, \tilde{H})$ , of problem (B.4) satisfy*

$$0 \leq \tilde{P} \leq \rho_1 e^{-\gamma t}, \quad 0 \leq \tilde{H} \leq \rho_2 e^{-(k_*^2 + \eta - m_1)t}. \tag{B.5}$$

*Proof* The linearity of the last two equations of the system (B.4) allows us to solve them in a straightforward way. In fact, by using the separation variables method for solving the equation for  $H$ , we obtain

$$\tilde{H}(t, \vec{x}) = \sum_{k \in \mathbb{Z}_+^2} c_k^h \exp(-(k^2 + \eta - m_1)t) X_k(\vec{x}),$$

where  $c_k^h$  are the Fourier expansion coefficients of the function  $h_0$  in terms of the eigenfunctions,  $X_k(\vec{x})$ , of the corresponding linear Sturm–Liouville problem

$$D_2 \Delta H + k^2 H = 0 \quad \text{in } \mathcal{R}, \quad \frac{\partial H}{\partial n} = 0 \quad \text{on } \partial \mathcal{R},$$

that is,

$$h_0(\vec{x}) = \sum_{k \in \mathbb{Z}_+^2} c_k^h X_k(\vec{x}),$$

where  $k^2 := k_1^2 + k_2^2$ . Hence, by choosing the main eigenvalue  $k^*$ , using the positivity and continuity of  $h_0(\vec{x})$  and Parseval’s identity, we find  $\rho_2 > 0$  (indeed,  $\sum_{k \in \mathbb{Z}_+^2} c_k^h < \rho_2$ ) and then a bound for  $\tilde{H}$ , as required.

Following a similar treatment, one can establish the existence of the bound  $\rho_1$ . In fact, by writing down the expression for  $\tilde{H}$  in the equation for  $P$  in (B.4), using the linearity of such equation we obtain  $\tilde{P}$ . Thus, let us denote by  $c_k^p$  the corresponding coefficients of the series representation for  $\tilde{P}$ , then we have  $\sum_{k \in \mathbb{Z}_+^2} c_k^p < \rho_1$ ; therefore the appropriate bound for  $\tilde{P}$  follows. Consequently, as had been claimed, the bounds are valid for all  $\{t > 0\} \times \mathcal{R}$ . Note that the bounds for  $\tilde{H}$  and  $\tilde{P}$  are valid whenever the inequality  $0 < \gamma < k^2 + \eta - m_1$  holds.  $\square$

Now, let us consider the equation for  $A$  in (B.4). Indeed, this one has two homogeneous and stationary solutions:  $A_1^*(t, \vec{x}) \equiv 0$  and  $A_2^*(t, \vec{x}) \equiv K$ . In order to determine their stability, we consider the following problem:

$$\begin{aligned}
 -D_1 \Delta A + \vec{v} \cdot \nabla A &= A \left( 1 - \frac{A}{K} \right), \quad \text{on } \mathcal{R}, \\
 \frac{\partial A}{\partial n} &= 0 \quad \text{on } \partial \mathcal{R}.
 \end{aligned}
 \tag{B.6}$$

Hence, we define the functional space,  $\mathcal{H}$ , whose elements are square integrable functions on  $\mathcal{R}$  satisfying homogeneous Neumann boundary conditions, i.e.,

$$\mathcal{H} := \left\{ u \in \mathcal{L}^2(\mathcal{R}) \mid \frac{\partial u}{\partial n} = 0 \text{ on } \partial \mathcal{R} \right\},
 \tag{B.7}$$

where the inner product

$$\langle u, v \rangle := \int_{\mathcal{R}} u(\vec{x})v(\vec{x}) \, d\vec{x},$$

is introduced. We also define the operator  $L : \mathcal{H} \rightarrow C(\mathbb{R})$  such that  $L := -D_1 \Delta + \vec{v} \cdot \nabla$ . In these terms, the problem (B.6) can be reformulated as the following nonlinear eigenvalue problem:

$$LA = A \left( 1 - \frac{A}{K} \right), \quad \text{on } \mathcal{H}.
 \tag{B.8}$$

As can be verified,  $L$  is an elliptic and hermitian operator. Therefore, its eigenvalues are real numbers and the corresponding set of eigenfunctions form an orthonormal basis of  $\mathcal{H}$ .

Now, let  $\varphi$  be the eigenfunction of  $L$  corresponding to its main eigenvalue,  $\lambda$ . By multiplying both sides of (B.8) by  $\varphi$  and integrating over  $\mathcal{R}$ , we obtain

$$\lambda \langle A, \varphi \rangle = \langle A, L\varphi \rangle = \langle LA, \varphi \rangle = \left\langle A \left( 1 - \frac{A}{K} \right), \varphi \right\rangle,$$

which can be written down in the following simple way:

$$(\lambda - 1) \langle A, \varphi \rangle = -\frac{1}{K} \langle A^2, \varphi \rangle,
 \tag{B.9}$$

which implies that

$$\lim_{t \rightarrow \infty} A(t, \vec{x}) = \begin{cases} 0 & \text{for } \lambda \geq 1, \\ K & \text{for } \lambda < 1. \end{cases}$$

However, because of the homogeneous Neumann boundary conditions, the main eigenvalue  $\lambda$  must be zero and the corresponding eigenfunction must be  $\varphi = 1$ .

Hence, the solution,  $A$ , for problem (B.6) is uniformly bounded in  $\mathcal{R}$  and satisfies

$$\lim_{t \rightarrow \infty} A(t, \vec{x}) = K. \quad (\text{B.10})$$

Therefore, the vectors  $\hat{u} \equiv (\tilde{A}, \tilde{P}, \tilde{H})$  and  $\check{u} \equiv (0, 0, 0)$ , are supersolution and subsolution for the system (B.1), respectively, as can be verified straightforwardly. Then by using Theorem 8.1 in Pao (1992), there exists a unique no negative solution,  $(a(t, \vec{x}), p(t, \vec{x}), h(t, \vec{x}))$ , for the problem (B.1) satisfying

$$(0, 0, 0) \leq (a(t, \vec{x}), p(t, \vec{x}), h(t, \vec{x})) \leq (\tilde{A}(t, \vec{x}), \tilde{P}(t, \vec{x}), \tilde{H}(t, \vec{x})), \quad (\text{B.11})$$

for all  $(t, \vec{x}) \in \mathbb{R}_+ \times \mathcal{R}$ .

Furthermore, from (B.5) follows

$$(a(t, \vec{x}), p(t, \vec{x}), h(t, \vec{x})) \leq (A, \rho_1 e^{-\gamma t}, \rho_2 e^{-(k^2 + \eta - m_1)t}), \quad (\text{B.12})$$

for all  $\{t > 0\} \times \mathcal{R}$ . Additionally, if  $t \rightarrow \infty$ , the following inequality holds:

$$(0, 0, 0) \leq (a(t, \vec{x}), p(t, \vec{x}), h(t, \vec{x})) \leq (K, 0, 0),$$

whenever  $k^2 + \eta > m_1$ . In the case  $m_1 \rightarrow k^2 + \eta$ , we have

$$(0, 0, 0) \leq (a(t, \vec{x}), p(t, \vec{x}), h(t, \vec{x})) \leq (K, \rho_1, \rho_2).$$

Collecting all the above results, what we have really proven is the global existence of solution for the problem (8) and its asymptotic behavior as well. We state it as follows.

**Theorem B.1** *Given the initial conditions  $(a_0(\vec{x}), p_0(\vec{x}), h_0(\vec{x})) \geq (0, 0, 0)$ , the problem (B.1), has a unique global solution  $(a(t, \vec{x}), p(t, \vec{x}), h(t, \vec{x}))$ , satisfying (B.12). This solution converges to  $(K, 0, 0)$  if  $t \rightarrow \infty$  and  $k^2 + \eta > m_1$ . In case  $m_1 \rightarrow k^2 + \eta$ , then the solution converges to  $(K, \rho_1, \rho_2)$ .*

*Remark* Note that previous theorem tells us that the problem (8) has bounded and positive solutions for all  $(t, \vec{x}) \in \mathbb{R}_+ \times \mathcal{R}$ .

## References

- Alt, W. (1985). Models for mutual attraction and aggregation of motile individuals. In *Lecture notes in biomathematics* (Vol. 57, pp. 33–38).
- Arrowsmith, D. K., & Place, C. M. (1998). *Dynamical systems. Differential equations, maps, and chaotic behavior*. London: Chapman and Hall.
- Boucher, D. H. (1982). *The biology of mutualism*. Oxford: Oxford University Press.
- Collings, J. B. (1997). The effect of the functional response on the bifurcation behaviour of a mite predator-prey interaction model. *J. Math. Biol.*, *36*, 149–168.
- Couzin, I. D., & Krause, J. (2003). Self-organization and collective behaviour in vertebrates. *Adv. Study Behav.*, *32*, 1–75.
- Crowley, M. J. (1992). *Natural enemies: The population biology of predators, parasites, and disease*. Oxford: Blackwell Scientific Publications.

- García-Ramos, G., Sánchez-Garduño, F., & Maini, P. K. (2000). Dispersal can sharpen parapatric boundaries in a spatially varying environment. *Ecology*, *81*(3), 749–760.
- Hanski, I. (1997). Metapopulation dynamics: From concepts and observations to predictive models. In I. A. Hanski & M. E. Gilpin (Eds.), *Metapopulation biology* (pp. 69–91). San Diego: Academic Press.
- Hanski, I. (1999). *Metapopulation ecology*. New York: Oxford University Press.
- Holmes, E. E., Lewis, M. A., Banks, J. E., & Veit, R. R. (1994). Partial differential equations in ecology: Spatial interactions and population. *Ecology*, *75*(1), 17–29.
- Jang, S. R. (2002). Dynamics of herbivore-plants-pollinator models. *J. Math. Biol.*, *44*, 129–149.
- Kierstead, H., & Slobodkin, L. B. (1953). The size of water masses containing plankton blooms. *J. Mar. Res.*, *12*, 141–147.
- Kot, M. (2001). *Elements of mathematical ecology*. Cambridge: Cambridge University Press.
- Kot, M., & Schaffer, W. M. (1986). Discrete-time growth dispersal models. *Math. Biosci.*, *80*, 109–136.
- Kuznetsov, Y. A. (2004). *Applied mathematical series: Vol. 112. Elements of applied bifurcation theory*. Berlin: Springer.
- Levin, S. A., & Segel, L. A. (1976). Hypothesis for origin of planktonic patchiness. *Nature*, *259*, 659.
- Malchow, H., Petrovskii, S. V., & Venturino, E. (2007). *Spatiotemporal patterns in ecology and epidemiology: Theory, models and simulation*. Boca Raton: Chapman and Hall/CRC.
- Market, P. A. (2002). Metapopulations. In H. A. Mooney & J. G. Canadell (Eds.), *The Earth system: Biological and ecological dimensions of global environmental change* (Vol. 2, pp. 411–420). Chichester: Wiley.
- May, R. M., & Southwood, T. R. E. (1990). Introduction. In B. Shorrocks & I. R. Swingland (Eds.), *Living in a patchy environment* (pp. 1–22). Oxford: Oxford University Press.
- Mimura, M., Nishiura, Y., & Yamaguti, M. (1979). Some diffusive prey and predator systems and their bifurcation problem. *Ann. N.Y. Acad. Sci.*, *316*, 490–510.
- Molofsky, J., & Bever, J. D. (2004). A new kind of ecology? *Bioscience*, *54*(5), 440–446.
- Muratov, C. B., & Osipov, V. V. (1996). Scenarios of domain patterns in a reaction-diffusion system. *Phys. Rev. E*, *54*, 4860.
- Murray, J. D. (2003). *Mathematical biology II: Spatial models and biomedical applications*. Berlin: Springer.
- Okubo, A. (1986). Dynamical aspects of animal grouping: Swarms, schools, and herds. *Adv. Biophys.*, *22*, 1–94.
- Okubo, A., & Levin, S. A. (2001). *Diffusion and ecological problems, modern perspective*. Berlin: Springer.
- Pao, C. V. (1992). *Nonlinear parabolic and elliptic equations*. New York: Plenum Press.
- Quilantán, I. (2010). *Dinámica espacio-temporal de una interacción polinizador-planta-herbívoro*. MSc Thesis on Applied Mathematics, DACB, UJAT, México.
- Sánchez-Garduño, F. (2001). Continuous density-dependent diffusion modelling in ecology: A review. *Recent Res. Ecol.*, *1*, 115–127.
- Sánchez-Garduño, F., & Breña-Medina, V. (2010). Existence, positiveness and boundness of solutions in a pollinator-plant-herbivore mathematical model. In preparation.
- Sánchez-Garduño, F., Maini, P. K., & Pérez-Velázquez, J. (2010). A nonlinear degenerate equation for direct aggregation and traveling wave dynamics. *Discrete Contin. Dyn. Syst., Ser. B*, *13*(2), 455–487.
- Segel, L. A., & Jackson, J. L. (1972). Dissipative structure: An explanation and an ecological example. *J. Theor. Biol.*, *37*, 545–559.
- Skellam, J. G. (1951). Random dispersal in theoretical populations. *Biometrika*, *38*, 196–218.
- Skellam, J. G. (1973). The formulation and interpretation of mathematical models of diffusory processes in population biology. In M. S. Batchellet et al. (Eds.), *The mathematical theory of the dynamics in biological populations*. New York: Academic Press.
- Soberón, J. M., & Martínez del Río, C. (1981). The dynamics of a plant-pollinator interaction. *J. Theor. Biol.*, *91*, 363–378.
- Steele, J. H. (1974). Spatial heterogeneity and population stability. *Nature*, *248*, 83.
- Turchin, P., & Kareiva, P. (1989). Aggregation in *aphis varians*: An effective strategy for reducing risk. *Ecology*, *70*(4), 1008–1016.
- Turchin, P. (1998). *Quantitative analysis of movement: Population redistribution in animals and plants*. Sunderland: Sinauer.
- Turing, A. M. (1952). The chemical basis of morphogenesis. *Philos. Trans. R. Soc. Lond. B*, *237*, 37–72.
- Velázquez, G. (2008). *Dinámica temporal de una interacción polinizador-planta-herbívoro*. MSc Thesis on Applied Mathematics, DACB, UJAT, México.